



CERN-EP-2021-083
10 May 2021

Investigating the role of strangeness in baryon–antibaryon annihilation at the LHC

ALICE Collaboration*

Abstract

Annihilation dynamics plays a fundamental role in the baryon–antibaryon interaction ($B\bar{B}$) at low-energy and its strength and range are crucial in the assessment of possible baryonic bound states. Experimental data on annihilation cross sections are available for the $p\bar{p}$ system but not in the low relative momentum region. Data regarding the $B\bar{B}$ interaction with strange degrees of freedom are extremely scarce, hence the modeling of the annihilation contributions is mainly based on nucleon–antinucleon ($N\bar{N}$) results, when available. In this letter we present a measurement of the $p\bar{p}$, $p\bar{\Lambda} \oplus \bar{p}\Lambda$ and $\Lambda\bar{\Lambda}$ interaction using correlation functions in the relative momentum space in high-multiplicity triggered pp collisions at $\sqrt{s} = 13$ TeV recorded by ALICE at the LHC. In the $p\bar{p}$ system the couplings to the mesonic channels in different partial waves are extracted by adopting a coupled-channel approach with recent χ EFT potentials. The inclusion of these inelastic channels provides good agreement with the data, showing a significant presence of the annihilation term down to zero momentum. Predictions obtained using the Lednický–Lyuboshits formula and scattering parameters obtained from heavy-ion collisions, hence mainly sensitive to elastic processes, are compared with the experimental $p\bar{\Lambda} \oplus \bar{p}\Lambda$ and $\Lambda\bar{\Lambda}$ correlations. The model describes the $\Lambda\bar{\Lambda}$ data and underestimates the $p\bar{\Lambda} \oplus \bar{p}\Lambda$ data in the region of momenta below 200 MeV/c. The observed deviation indicates a different contribution of annihilation channels to the two systems containing strange hadrons.

arXiv:2105.05190v2 [nucl-ex] 5 Dec 2022

© 2021 CERN for the benefit of the ALICE Collaboration.

Reproduction of this article or parts of it is allowed as specified in the CC-BY-4.0 license.

*See Appendix B for the list of collaboration members

1 Introduction and physics motivation

The baryon–antibaryon interaction ($B\text{--}\bar{B}$) is dominated at low energies by annihilation processes, in which transitions from a state, typically composed of only mesons, to a $B\text{--}\bar{B}$ state and vice versa are occurring. Since the first measurement of the proton–antiproton ($p\text{--}\bar{p}$) cross section [1], a rich sample of experimental data has become available, mainly in the nucleon–antinucleon ($N\text{--}\bar{N}$) sector. Low-energy scattering experiments [2–4] delivered data on the total cross section, on the elastic ($p\bar{p} \rightarrow p\bar{p}$) and charge-exchange ($p\bar{p} \rightarrow n\bar{n}$) cross sections, down to laboratory momenta $p_{\text{lab}} \approx 200 \text{ MeV}/c$. Measurements of the annihilation cross section reach even lower momenta but are affected by significant uncertainties and in particular the momentum region close to the $p\text{--}\bar{p}$ threshold is currently lacking any experimental constraint. This region is however of particular interest for the theoretical modeling of $p\text{--}\bar{p}$ interaction since the interplay between the Coulomb and the annihilation dynamics is dominant.

At threshold, measurements of the energy level shifts and widths of $p\text{--}\bar{p}$ atoms [5] enabled the extraction of the spin-averaged scattering parameters, confirming a non-zero imaginary part of the scattering length related to the presence of inelastic channels due to the annihilation processes.

Great effort was made in the theoretical description of the short-range interaction (below 1 fm) of $p\text{--}\bar{p}$ systems since a stronger elastic attraction, with respect to the $p\text{--}p$ case, is expected to occur in some spin-isospin channels, leading to predictions of the existence of bound states (baryonia) [5, 6]. Findings of broad resonances and enhancements in the $p\text{--}\bar{p}$ invariant mass [7–10] measured in the decays of charmed and bottom mesons were reported but no clear evidence of such bound states has been found yet. A precise understanding of the annihilation dynamics is required to assess the existence of such states since the bound spectrum could be washed out by the $B\text{--}\bar{B}$ annihilation part of the interaction. The annihilation term in the $N\text{--}\bar{N}$ sector is typically described in chiral-effective potentials [11], meson-exchange [12–14] and quark models [15] by means of phenomenological optical potentials and contact interactions with parameters to be fixed from the available data. The search for baryonia states for $B\text{--}\bar{B}$ systems in the strangeness sector with hyperons (Y) and antihyperons (\bar{Y}), e.g. $N\text{--}\bar{Y}$, $Y\text{--}\bar{Y}$ is even more challenging since the experimental informations are very scarce, with $p\bar{p} \rightarrow \Lambda\bar{\Lambda}$ being the only measured strangeness exchange process [5]. Consequently, the modeling of the annihilation for systems as $Y\text{--}\bar{Y}$ (e.g. $\Lambda\text{--}\bar{\Lambda}$) is mainly based on the $N\text{--}\bar{N}$ interaction [16–19]. Measurements of the $p\text{--}\bar{\Lambda}$ invariant mass spectra in photoproduction processes $\gamma p \rightarrow \Lambda\bar{\Lambda}p$ will become available in the next years [20], but currently no experimental informations neither theoretical predictions are present for $B\text{--}\bar{B}$ interactions involving a nucleon (antinucleon) and an antihyperon (hyperon) such as $p\text{--}\bar{\Lambda}$.

The study of annihilation in $B\text{--}\bar{B}$ systems with strangeness is also of great interest for the modeling of the re-scattering phase in heavy-ion collisions (HIC). Several observables as particle spectra and yields strongly depend on the processes occurring at this stage of the HIC evolution, the $B\text{--}\bar{B}$ annihilation processes above all. Currently in HIC, the annihilation interaction for pairs containing strangeness is either modeled assuming scattering parameters similar to $p\text{--}\bar{p}$ or with an ad-hoc suppression of the cross section with respect to the $p\text{--}\bar{p}$ counterpart [21, 22].

The present theoretical understanding of the $B\text{--}\bar{B}$ interaction requires additional precise data particularly in the low-momentum region, where the inelastic contributions from annihilation are relevant. This would shed light on the presence of baryonia bound states and on how the annihilation dynamics changes for systems with strangeness.

A step in this direction has recently been achieved with the measurements of two-particle correlations in the momentum space for $p\text{--}\bar{p}$, $p\text{--}\bar{\Lambda}$ and $\Lambda\text{--}\bar{\Lambda}$ pairs performed in ultra-relativistic Pb–Pb collisions at LHC [23]. The extracted spin-averaged scattering parameters are in agreement for all $B\text{--}\bar{B}$ pairs indicating that the annihilation part for all $B\text{--}\bar{B}$ pairs is similar at the same relative momentum. The $p\text{--}\bar{\Lambda}$ pairs were also measured in Au–Au collisions at RHIC [24], but these results might be biased by the neglected residual correlations [21]. Measurements of hadron–hadron correlations have been performed in small colliding systems such as pp and p–Pb, and they delivered the most precise data on baryon–baryon and meson–baryon pairs, enabling access to the short-range strong interaction [25–31]. This kind

of measurements in pp collisions can probe inter-particle distances of around 1 fm and are sensitive to the presence of inelastic channels, below and above threshold [27, 32, 33].

In this letter we present the measurements of the correlation functions of $p\bar{p}$, $p\bar{\Lambda} \oplus \bar{p}\Lambda$ and $\Lambda\bar{\Lambda}$ pairs in pp collisions at $\sqrt{s} = 13$ TeV with the ALICE detector [34, 35]. To better constrain the interaction, a differential analysis in pair-transverse-mass (m_T) intervals has been performed for the $p\bar{\Lambda} \oplus \bar{p}\Lambda$ and $\Lambda\bar{\Lambda}$ pairs. The work presented in this Letter delivers the most precise data at low momenta for $p\bar{p}$, $p\bar{\Lambda}$ and $\Lambda\bar{\Lambda}$ systems and provides additional experimental constraints for the modeling of the B– \bar{B} interaction.

2 Data analysis

The main ALICE subdetectors [34, 35] used in this analysis are: the V0 detectors [36] used as trigger detectors, the Inner Tracking System (ITS) [37], the Time Projection Chamber (TPC) [38] and the Time-of-Flight (TOF) detector [39]. The last three are used to track and identify charged particles. The high-multiplicity (HM) sample used in this analysis corresponds to 0.17% of all inelastic pp collisions with at least one measured charged particle within $|\eta| < 1$ (referred to as INEL>0) [29, 30]. The corresponding HM trigger is defined by coincident hits in both V0 detectors synchronous with the collider bunch crossing and by requiring as well that the sum of the measured signal amplitudes in the V0 exceeds a multiple of the average value in minimum bias collisions. The rejection of pile-up events have been applied by evaluating the presence of additional event vertices as done in [29, 31] and a total of 1.0×10^9 HM events are selected.

Protons and antiprotons are reconstructed using the procedure described in Refs. [29, 31]. Primary protons and antiprotons are selected in the transverse momentum range $0.5 < p_T < 4.05$ GeV/c and pseudorapidity $|\eta| < 0.8$. A minimum of 80 out of the 159 available spatial points (hits) inside the TPC are required to obtain high-quality tracks. The TPC and TOF detectors select p (\bar{p}) candidates by the deviation n_σ between the signal hypothesis for the considered particle and the experimental measurement, normalized by the detector resolution σ [29, 31]. For candidates with $p < 0.75$ GeV/c, the particle identification (PID) is performed with the TPC only. For larger momenta, the PID information of TPC and TOF are combined. The candidates are accepted if their $|n_\sigma| < 3$. To reject non-primary protons (antiprotons), the distance of closest approach (DCA) of the candidates tracks to the primary vertex is required to be less than 0.1 cm in the xy -plane and less than 0.2 cm along the beam axis. Contributions of secondary (anti)protons stemming from weak decays and misidentified candidates are extracted using Monte Carlo (MC) template fits to the measured distance of closest approach (DCA) distributions of the to the primary vertex [25]. The resulting p (\bar{p}) purity is 99.4% (98.9%). The corresponding fraction of primary particles is 82.2% (82.3%).

The reconstruction of the Λ ($\bar{\Lambda}$) candidates, via their weak decay $\Lambda \rightarrow p\pi^-$ ($\bar{\Lambda} \rightarrow \bar{p}\pi^+$) [40], is performed following the procedures described in Refs. [29, 31]. A final selection is applied based on the reconstructed invariant mass [29, 31]. The obtained Λ ($\bar{\Lambda}$) purity is 95.2% (96.1%). Primary and secondary contributions for Λ and $\bar{\Lambda}$ are extracted in a similar way as for protons, via fits to the cosine of the pointing angle distributions using MC templates. The fraction of primary Λ ($\bar{\Lambda}$) hyperons is about 57%. Secondary contributions from weak decays of neutral and charged Ξ baryons amount to 22%. The remaining fractions are attributed to Σ^0 ($\bar{\Sigma}^0$) particles. Systematic uncertainties on the data are evaluated by varying the kinematic and topological selection criteria following [29, 31].

3 Analysis of the correlation function

The main observable in the analysis presented here is the two-particle correlation function $C(k^*)$, which depends on the relative momentum k^* evaluated in the pair rest frame [25]. In femtoscopy measurements, the final state is fixed to the measured particle pair and the corresponding correlation function is sensitive to all the available initial, elastic and inelastic, channels produced in the collision [32, 33]. For the study

of the $B\bar{B}$ interaction, the single-channel Koonin-Pratt equation [41] has to be modified in order to accommodate the inelastic contributions stemming from the annihilation channels [32, 33].

Assuming that the interaction of the pair in the final state i is affected by the inelastic channels j , the Koonin-Pratt formula is modified by the introduction of an additive term related to the processes $j \rightarrow i$ [32, 33, 42]:

$$C_i(k^*) = \int d^3r^* S(r^*) |\psi_i(k^*, r^*)|^2 + \sum_{j \neq i}^N \omega_j \int d^3r^* S(r^*) |\psi_j(k^*, r^*)|^2. \quad (1)$$

The first integral on the right-hand side describes the elastic contribution where initial and final state coincide, while the second integral is responsible for the remaining inelastic processes $j \rightarrow i$. This last integral depends on two main ingredients: the wave function $\psi_j(k^*, r^*)$ for channel j going to the final state i and the conversion weights ω_j . These latter quantities can be written as $\omega_j = \omega_j^s \times \omega_j^{\text{prod}}$, in which ω_j^{prod} is related to the amount of j pairs produced in the initial collision and kinematically available to be converted to the final measured state. Quantitative estimates on these production weights can be obtained combining thermal model calculations of particle yields [43] with kinematics constraints from transport models [44]. If the assumed inelastic wave function $\psi_j(k^*, r^*)$ is properly accounting for the coupling strength, the corresponding ω_j^s weight is equal to unity.

Recent femtoscopic measurements by the ALICE Collaboration performed on K^-p pairs in pp [27] and in Pb–Pb collisions [45] showed that by changing the colliding system, and hence the size of the emitting source $S(r^*)$, the effects on the $C(k^*)$ due to the inelastic contributions given by the last term in Eq. (1) are enhanced or suppressed. The wave functions $\psi_j(k^*, r^*)$ related to the inelastic channels are localized at distances r^* approximately below 1.5–2 fm and equal to zero above. Hence, performing femtoscopic measurements with a large emitting source, as it occurs in central heavy-ion collisions (r^* above 5 fm), results in a correlation function mainly dominated by the elastic contribution, given by the first term of Eq. (1). For this reason, the $C(k^*)$ measured in Pb–Pb can be modeled with the single-channel Lednický–Lyuboshits formula [42] assuming a complex scattering length f_0 , in which the imaginary part $\mathcal{I}f_0$ accounts for an average inelastic contribution from all j channels.

These inelastic contributions become more relevant when performing the same measurement in small colliding systems as pp, where the emitting source size is of the order of 1 fm [46] and the modeling of the $C(k^*)$ requires the knowledge of the exact elastic $\psi_i(k^*, r^*)$ and inelastic $\psi_j(k^*, r^*)$ wave functions obtained from the solution of a coupled-channel approach [46]. If the theoretical modeling of the interaction properly accounts for the inelastic channels ($\omega_j^s = 1$), the use of the modified Koonin-Pratt formula in Eq. (1) with a proper estimate of the production weights ω_j^{prod} will describe the data in both small and large colliding systems as shown in [45] for the K^-p system. The use of the single-channel Lednický–Lyuboshits model will only be applicable if the wave functions $\psi_j(k^*, r^*)$ would be strongly suppressed, corresponding to a very weak coupling to the inelastic channels.

The $B\bar{B}$ interaction investigated in this work is less known with respect to the K^-p case in [27, 45], hence two different approaches have been used to calculate the theoretical correlation for the $p\bar{p}$ and the $\Lambda\bar{\Lambda}$, $p\bar{\Lambda}$ pairs, respectively. For both approaches the CATS framework is used [47].

The genuine $p\bar{p}$ correlation is modeled either by assuming a Coulomb-only interaction or by also including a strong interaction from $N\bar{N}$ chiral effective (χ EFT) potentials at next-to-next-to-next-to-leading order (N^3 LO) [11]. The $p\bar{p}$ wave functions, available for S ($^1S_0, ^3S_1$) and P ($^1P_1, ^3P_0, ^3P_1, ^3P_2$) partial-waves (PW), have been evaluated within a coupled-channel formalism in which only the coupling to the charge-exchange $n\bar{n}$ channel is explicitly included. The formula in Eq. (1) is used for the genuine $p\bar{p}$ correlation function with the chiral wave functions for the elastic $i = p\bar{p}$ and the charge-exchange channel $j = n\bar{n}$ [11]. The wave functions $\psi_{X \rightarrow p\bar{p}}^{\text{PW}}$, accounting for the multi-meson annihilation channels $j = X$, are not currently available. The annihilation contribution is implicitly present in the χ EFT potentials in [11] since the parameters of the model are constrained to the most-recent partial-wave analysis

on the available $p\bar{p}$ and $N\bar{N}$ cross sections [4].

The Migdal-Watson approximation [48] is used as an approximate way to explicitly include the additional $j = X$ annihilation channels. This approximation relies on the fact that these X multi-meson channels open below the $p\bar{p}$ threshold and hence the momentum dependence of the annihilation potential $V_{X\rightarrow p\bar{p}}$ around the $p\bar{p}$ threshold can be neglected. The wave functions $\psi_{X\rightarrow p\bar{p}}^{\text{PW}}$ for each PW can be rewritten in terms of the elastic component as $\omega_{\text{PW}}\psi_{p\bar{p}\rightarrow p\bar{p}}^{\text{PW}}$, with the weights ω_{PW} to be determined from data. These latter weights are directly connected to the conversion weights ω_j in Eq. (1) with the strong coupling term ω_j^s extended to the different PW states. A detailed estimate of the yields and kinematics of the annihilation channels (ω_j^{prod}), necessary to isolate the strong coupling term in each PW, is not trivial since it involves contributions stemming from multi-pions channels and it should include also intermediate states of resonances strongly decaying into pions. For this reason, the extracted weights ω_{PW} in this work contain informations not only on the coupling strength of the mesonic channels to $p\bar{p}$, but also on the abundances of the contributing multi-meson channels produced in the initial state.

The modeled correlation function reads [33]:

$$\begin{aligned} C_{p\bar{p}}(k^*) &= \int S(r^*)|\psi_{p\bar{p}\rightarrow p\bar{p}}|^2 d^3 r^* + \int S(r^*)|\psi_{n\bar{n}\rightarrow p\bar{p}}|^2 d^3 r^* + \sum_{\text{PW}} \rho_{\text{PW}} \omega_{\text{PW}} \int S(r^*)|\psi_{p\bar{p}\rightarrow p\bar{p}}^{\text{PW}}|^2 d^3 r^* \\ &= C_{p\bar{p}\rightarrow p\bar{p}}(k^*) + C_{n\bar{n}\rightarrow p\bar{p}}(k^*) + \sum_{\text{PW}} C_{X\rightarrow p\bar{p}}^{\text{PW}}(k^*). \end{aligned} \quad (2)$$

The first and second terms describe the elastic and $n\bar{n}$ contributions, while the last term accounts for the annihilation channels. The degeneracy in spin and angular momentum is embedded in the statistical factors ρ_{PW} . To reduce the number of ω_{PW} weights to be fitted, a study on the shape of the single inelastic correlation terms $C_{X\rightarrow p\bar{p}}^{\text{PW}}(k^*)$ is performed in each partial wave. The correlations with a different profile in k^* are selected, allowing to determine three representative contributions: the 1S_0 for S states, the 1P_1 and 3P_0 for P states.

For the two systems containing strangeness, $p\bar{\Lambda}$ and $\Lambda\bar{\Lambda}$, no theoretical wave functions are currently available, hence the single-channel Lednický–Lyuboshits analytical formula with a complex scattering length f_0 is used to evaluate the theoretical correlations [23, 42]. As mentioned above, in this single-channel approach, only the elastic contributions are explicitly accounted for in the $\mathcal{R}f_0$, corresponding to the first term in Eq. 1. The imaginary part $\mathcal{I}f_0$ accounts for an average over all the inelastic contributions of the $B\bar{B}$ interaction, mainly dominated by annihilation. The same approach has been used in the ALICE femtoscopic measurements in Pb–Pb collisions [23], which delivered the only available scattering parameters on both the $p\bar{\Lambda}$ and $\Lambda\bar{\Lambda}$ interaction. For the latter, theoretical predictions are available [16], providing values for the scattering parameters compatible with the ALICE Pb–Pb results [23].

The emitting source in Eq. 1 can be determined as a function of the pair-transverse-mass m_T with a data-driven model based on proton-proton correlations [31]. This allows us to investigate the interaction for different particle pairs. The properties of the underlying interaction in $p\bar{\Lambda}$ and $\Lambda\bar{\Lambda}$ systems do not depend on m_T and can hence be better constrained using a m_T differential analysis. Considering the available sample, 6 and 3 m_T intervals are used for the $p\bar{\Lambda}$ and $\Lambda\bar{\Lambda}$ measured correlations, respectively. These experimental correlations are compared, in each m_T interval, to the Lednický–Lyuboshits model by assuming at first the scattering parameters obtained in the Pb–Pb analysis [23]. Secondly, a simultaneous fit for each pair in all the available m_T bins is performed leaving the $\mathcal{I}f_0$ to vary in order to test if a better agreement with the data is achieved. Further discussions on the two different fitting procedures can be found in the next section.

Experimentally, the correlation function is defined as

$$C(k^*) = \mathcal{N} \frac{N_{\text{SE}}(k^*)}{N_{\text{ME}}(k^*)} \xrightarrow{k^* \rightarrow \infty} 1. \quad (3)$$

Here $N_{\text{SE}}(k^*)$ is the distribution of pairs measured in the same event, $N_{\text{ME}}(k^*)$ is the reference distribution of uncorrelated pairs sampled from different (mixed) events and \mathcal{N} is a normalization parameter determined by requiring that particle pairs with large k^* are not correlated. The mixed-event sample is obtained by pairing particles stemming from events with a similar number of charged particles at midrapidity and a close-by primary vertex position along the beam direction as done in [27, 29, 30]. The correlation functions of baryon–antibaryon and antibaryon–baryon pairs are combined to enhance the statistical significance for the $p\text{--}\bar{\Lambda}$ pairs, hence in the following $p\text{--}\bar{\Lambda}$ denotes the sum $p\text{--}\bar{\Lambda} \oplus \bar{p}\text{--}\Lambda$. The $p\text{--}\bar{p}$, $p\text{--}\bar{\Lambda}$ and $\Lambda\text{--}\bar{\Lambda}$ data are fitted with a total correlation function

$$C_{\text{tot}}(k^*) = N_D \times C_{\text{model}}(k^*) \times C_{\text{background}}(k^*), \quad (4)$$

where N_D is a normalization constant fitted to data. The default fit range is $0 < k^* < 500$ MeV/ c . The modeled $C_{\text{model}}(k^*) = 1 + \sum_i \lambda_i \times (C_i(k^*) - 1)$ includes the genuine ($i = p\text{--}\bar{p}, p\text{--}\bar{\Lambda}, \Lambda\text{--}\bar{\Lambda}$) correlation, estimated from Eq. 2 and using the Lednický–Lyuboshits model, and the residual secondary contributions weighted by the λ_i parameters [25]. The genuine contributions for $p\text{--}\bar{p}$, $p\text{--}\bar{\Lambda}$ and $\Lambda\text{--}\bar{\Lambda}$ amount to $\lambda_{p\text{--}\bar{p}} = 66.5\%$, $\lambda_{p\text{--}\bar{\Lambda}} = 45.8\%$ and $\lambda_{\Lambda\text{--}\bar{\Lambda}} = 30.9\%$, respectively. Residual contributions involving pairs measured in this work are modeled assuming the corresponding theoretical predictions mentioned above. Contributions involving $\Sigma^{\pm,0}$ ($\bar{\Sigma}^{\pm,0}$) and $\Xi^{\pm,0}$ ($\bar{\Xi}^{\pm,0}$) are considered to be constant in k^* due to the limited theoretical knowledge, and amount to 10.1%, 44.6% and 65.7% for $p\text{--}\bar{p}$, $p\text{--}\bar{\Lambda}$ and $\Lambda\text{--}\bar{\Lambda}$, respectively. A crosscheck on these residuals by assuming a strong interaction based on the scattering parameters extracted in Pb–Pb measurements [23] was performed and differences in the extracted results with respect to the constant assumption are found to be negligible.

A variation of $\pm 10\%$ to the upper limit of the default fit range is applied for evaluating the systematic uncertainties. Additionally, the systematic uncertainties related to the λ_i parameters are evaluated based on variations of the amount of secondary contributions to each measured particle species, where the largest source of uncertainty stems from the ratio $\Sigma^0 : \Lambda = 0.33 \pm 0.07$ [31, 43, 49–51]. In addition to the feed-down contributions, a correction for finite experimental momentum resolution has to be taken into account for a direct comparison with data [25].

The size of the emitting source employed in the calculation of $C_{\text{model}}(k^*)$ for the three $B\text{--}\bar{B}$ pairs is fixed from the data-driven analysis of $p\text{--}p$ pairs, which demonstrates the existence of a common Gaussian core as a function of m_T for all baryon–baryon pairs when contributions from short-lived strongly decaying resonances are properly included [31]. For the $p\text{--}\bar{p}$ pairs, the core source size at the corresponding $\langle m_T \rangle = 1.45$ GeV/ c^2 is $r_{\text{core}} = 1.06 \pm 0.04$ fm and the associated effective Gaussian source size is $r_0 = 1.22$ fm. The core radii for the $p\text{--}\bar{\Lambda}$ and $\Lambda\text{--}\bar{\Lambda}$ m_T bins presented in this letter are $r_{\text{core}}(\langle m_T \rangle = 1.75$ GeV/ c^2) = 0.95 ± 0.04 fm ($r_0 = 1.15$ fm) and $r_{\text{core}}(\langle m_T \rangle = 2.12$ GeV/ c^2) = 0.87 ± 0.04 fm ($r_0 = 1.11$ fm), respectively.

The second term in Eq. 4, $C_{\text{background}}(k^*)$, accounts for non-femtoscopic effects due to energy-momentum conservation at large k^* [25] and to minijet phenomena arising from hard processes at the parton level, largely present in the measurement of $B\text{--}\bar{B}$ correlations:

$$\begin{aligned} C_{\text{background}}(k^*) &= C_{\text{minijet}}(k^*) + C_{\text{baseline}}(k^*) \\ &= [w_C C_C(k^*) + (1 - w_C) C_{NC}(k^*)] + (a + bk^*). \end{aligned} \quad (5)$$

A data-driven approach is employed using PYTHIA 8.2 [52] to model the mini-jet part contained in $C_{\text{background}}(k^*)$. The particle production in such simulations is associated to two processes: particles stemming from a common parton (common ancestors), leading to the minijet component, and particles coming from different partons (non-common ancestors), responsible for the non-jet part. The $C_{\text{minijet}}(k^*)$ in Eq. (5) is given by a linear combination of the common ($C_C(k^*)$) and non-common ($C_{NC}(k^*)$) contributions weighted by a factor w_C and $(1 - w_C)$, respectively. The ancestor weight w_C is a free parameter in the fit of $C_{\text{tot}}(k^*)$ to the data. The common and non-common correlations obtained from PYTHIA 8.2 are fitted with a product of three Gaussian functions up to $k^* = 2500$ MeV/ c , providing good agreement with the simulated data. To account for remaining non-femtoscopic effects at large k^* [25], a linear baseline $C_{\text{baseline}}(k^*) = a + bk^*$ is added to the ancestors term in Eq. (5). The coefficients a and b are fixed by fitting $C_{\text{background}}(k^*)$ to the data in the region of $400 < k^* < 2500$ MeV/ c . The results for $p-\bar{p}$ pairs are shown in Fig. 1. The band represents the 1σ uncertainty associated to the template fitting. The shape of $C_{\text{background}}(k^*)$ agrees within uncertainties with the data in the region above $k^* \approx 200$ MeV/ c , where the non-flat behavior of minijet contributions is visible. A change of $\pm 10\%$ in this range and a quadratic polynomial are included to estimate the systematic uncertainty related to the total background. Similar results and conclusions are obtained for the $p-\bar{\Lambda}$ and $\Lambda-\bar{\Lambda}$ systems.

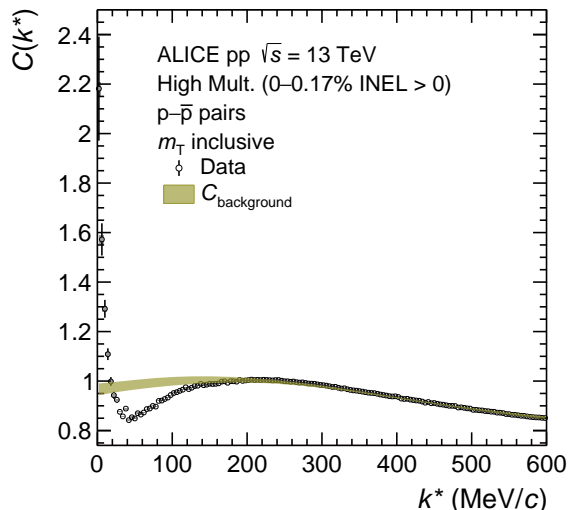


Figure 1: (Color online) Measured $p-\bar{p}$ correlation function (empty points) with statistical (line) and systematic (grey boxes) uncertainties. The band represents the $C_{\text{background}}(k^*)$ fit as described in the text.

4 Results

The correlation functions for $p-\bar{p}$ and for two representative m_T bins of $p-\bar{\Lambda}$ and $\Lambda-\bar{\Lambda}$ are shown in Fig. 2 and in Fig. 3, respectively. The results for the remaining m_T bins are presented in Figs. A.1, A.2 of Appendix A.1. The lower panels show the statistical deviation between data and model expressed in terms of numbers of standard deviation n_σ . The width of the band represents the total uncertainty of the fit. The grey boxes correspond to the systematic uncertainties of the data. They are maximal at the lowest k^* bin and amount to 1%, 4% and 10% for $p-\bar{p}$, $p-\bar{\Lambda}$ and $\Lambda-\bar{\Lambda}$ pairs, respectively. The $C_{p-\bar{p}}(k^*)$ correlation is compared first to a Coulomb-only interaction and secondly to a Coulomb + strong interaction from $N-\bar{N}$ χ EFT potentials with wave functions for the $n-\bar{n} \rightarrow p-\bar{p}$ process explicitly included [11]. Results for this latter scenario are obtained by evaluating the genuine $p-\bar{p}$ correlation in Eq. (2) with only the first two terms and shown in blue in Fig. 2. The opening of the $n-\bar{n}$ channel above threshold, expected as a cusp structure in the $C(k^*)$ at $k^* \approx 50$ MeV/ c , is not visible in agreement with the weak coupling

already measured in scattering experiments [4]. The chiral model underestimates the data in the region below 200 MeV/c and it cannot reproduce the enhancement above unity of the $C(k^*)$ as k^* approaches zero. This increase is not described either by assuming only the Coulomb attraction (green band), showing that annihilation is largely present close to threshold as $k^* \rightarrow 0$ MeV/c. The contributions to the $p\bar{p}$ correlation from the multi-meson annihilation channels, produced as initial states which feed into the measured $p\bar{p}$ system, are not explicitly accounted for in the chiral potential and hence the last term $\sum_{PW} C_{X \rightarrow p\bar{p}}^{PW}(k^*)$ in Eq.(2) is currently missing in the fit shown by the blue band.

The red band in Fig. 2 represents the results obtained from the explicit inclusion of the annihilation channels in the third term of Eq. (2) via the Migdal-Watson approximation. The corresponding fit provides a better description of the data in the low k^* region where annihilation is dominant. The extracted coupling weights ω_{PW} from this femtoscopic fit are $\omega_{S_0} = 1.19 \pm 0.10$ (stat) ± 0.19 (syst) and $\omega_{S_{P_0}} = 40.04 \pm 4.06$ (stat) ± 4.24 (syst), while ω_{P_1} is compatible with zero. The hierarchy of the coupling weights in the different PW agrees with the inelasticity parameters η obtained in the recent partial-wave analysis [4].

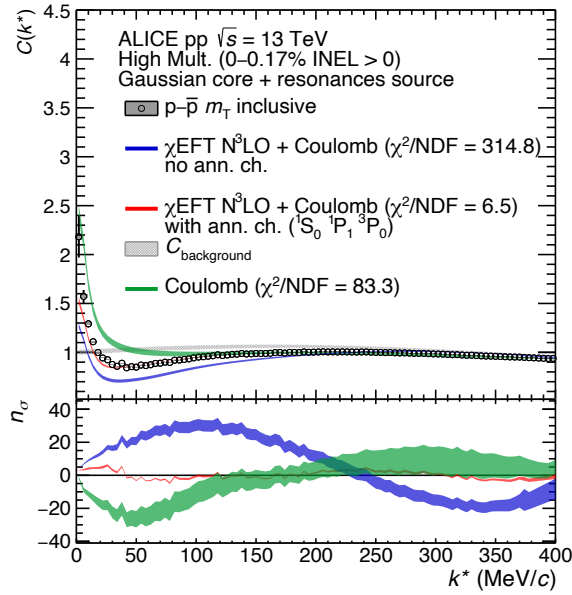


Figure 2: (Color online) Measured correlation function of $p\bar{p}$ pairs. Statistical (bars) and systematic (boxes) uncertainties are shown separately. The Coulomb only interaction is shown by the green band. The blue band represents the fit performed using $N^3\text{LO}$ χEFT potentials [11] with elastic and $n\bar{n}$ coupled-channel. The inclusion of annihilation channels is shown by the red band, along with the $C_{\text{background}}(k^*)$, multiplied by the normalization constant N_D obtained in the fit. The reported average χ^2/NDF is evaluated in the k^* interval $[0, 400]$ MeV/c and it includes correlations between the data points. Lower panel: n_σ deviation between data and model in terms of numbers of statistical standard deviations.

For the systems containing strangeness, the Migdal-Watson approach cannot be employed since only scattering parameters for the $p\bar{\Lambda}$ and $\Lambda\bar{\Lambda}$ interaction are available [23]. The values of $\mathcal{R}f_0$ and $\mathcal{I}f_0$ obtained in Pb–Pb measurements are employed in the Lednický–Lyuboshits analytical formula [23, 42] to model the $p\bar{\Lambda}$ and $\Lambda\bar{\Lambda}$ genuine correlation functions. In Fig. 3, the results obtained modeling the $p\bar{\Lambda}$ and $\Lambda\bar{\Lambda}$ theoretical correlations with the Lednický–Lyuboshits model described in Sec. 3 are shown. The first tested scenario assumes the scattering parameters extracted from Pb–Pb results [23] and the results are denoted by light green bands. It can be expected that if the direct contributions of the annihilation channels are negligible, the values extracted in Pb–Pb will reproduce well also the pp data in this analysis. As can be seen from the right panel in Fig. 3, this first approach reproduces the measured $\Lambda\bar{\Lambda}$ correlation function, with an average $\chi^2/\text{NDF} = 2.8$ evaluated in the k^* interval $[0, 400]$ MeV/c but it clearly underestimates the $p\bar{\Lambda}$ correlation data in the k^* region below 200 MeV/c. A similar

trend is observed when performing the fit to the $p\text{-}\bar{p}$ measured correlation with the Lednický–Lyuboshits approach used in the Pb–Pb results [23] as shown in Fig. A.3 in the Appendix A.2. The discrepancy hence, as in the $p\text{-}\bar{p}$ case, has to be attributed to a larger amount of annihilation channels feeding into the $p\text{-}\bar{\Lambda}$ system with respect to the $\Lambda\text{-}\bar{\Lambda}$ pairs. To validate this interpretation, a simultaneous fit in all the m_T bins is performed leaving free to vary the imaginary part of the scattering length $\mathcal{I}f_0$, accounting for inelastic channels, and the effective range d_0 . The negative real part of the scattering length $\mathcal{R}f_0$, indicating either a repulsive elastic interaction or a possible bound state, is kept fixed to the Pb–Pb results [23]. To reach a reasonable agreement of the model with $p\text{-}\bar{\Lambda}$ data, $\mathcal{I}f_0$ has to be increased by approximately a factor 5.3, while the change in the extracted d_0 is negligible. Such a discrepancy can be attributed to the failure of the single-channel Lednický–Lyuboshits model to properly accommodate the direct contribution of inelastic channels (last term in Eq. (1)). A similar fit is applied to the $\Lambda\text{-}\bar{\Lambda}$ system and values of $\mathcal{I}f_0$ and d_0 compatible with the Pb–Pb measurements are found, implying a negligible effect of the direct contribution of annihilation channels. The corresponding results are shown in Fig 3 (orange band), for $p\text{-}\bar{\Lambda}$ (left panel) and $\Lambda\text{-}\bar{\Lambda}$ (right panel). A similar trend is obtained in the remaining m_T intervals and shown in Appendix A.1.

The different results for the $p\text{-}\bar{\Lambda}$ and $\Lambda\text{-}\bar{\Lambda}$ systems may also be related to a different amount of initially produced multi-meson states feeding into the two $B\text{-}\bar{B}$ pairs. To substantiate this scenario, a study of the two-meson channel contributions ($\pi\bar{\pi}$, $\pi\bar{K}$) is performed using the EPOS transport model [44]. The fraction of two-mesons pairs $f_{2M\rightarrow B\bar{B}}$ produced in the initial collision and kinematically available to produce $B\text{-}\bar{B}$ pairs with low k^* is estimated. The latter is obtained by dividing the amount of meson-meson pairs initially produced, having a center-of-mass energy above the $B\text{-}\bar{B}$ threshold and leading to $B\text{-}\bar{B}$ pairs at low k^* , by the total number of produced two-meson pairs kinematically allowed to create the $B\text{-}\bar{B}$ pairs. Based on this study and considering these kinematics considerations, a similar amount ($\approx 6.4\%$) is found for $p\text{-}\bar{\Lambda}$ and $\Lambda\text{-}\bar{\Lambda}$ pairs, indicating that the above effect is related to the properties of the $p\text{-}\bar{\Lambda}$ and $\Lambda\text{-}\bar{\Lambda}$ interaction. To quantify the final relative amount of annihilation channels feeding to the $p\text{-}\bar{\Lambda}$ and $\Lambda\text{-}\bar{\Lambda}$ systems, the fractions have to be multiplied by the corresponding coupling constant g , obtained within an SU(3) Lagrangian by evaluating the trace of the meson–baryon interaction term [53]. Within this simplified calculations, the coupling strength for the $p\text{-}\bar{\Lambda}$ system is found to be approximately 3.3 times larger than for the $\Lambda\text{-}\bar{\Lambda}$ pairs.

The estimated contribution $g \times f_{2M\rightarrow B\bar{B}}$, although limited to only two-meson channels, for $p\text{-}\bar{\Lambda}$ pairs is found to be about 6 times larger than for $\Lambda\text{-}\bar{\Lambda}$ pairs, indicating a different annihilation contributions occurring in $p\text{-}\bar{\Lambda}$ and $\Lambda\text{-}\bar{\Lambda}$ interaction which is confirmed by the measured correlation functions in Fig. 3. These estimations, even though based on a qualitative approach, clearly indicates that the annihilation for the $\Lambda\text{-}\bar{\Lambda}$ interaction is present but it should not be largely dominant over the elastic part. More input from theory is needed in order to claim if such a condition is ideal for the formation of bound-states in the $\Lambda\text{-}\bar{\Lambda}$ system. The results for the $p\text{-}\bar{\Lambda}$ system, however, clearly point to a much larger presence of the annihilation channels, which might reduce the possibility to create baryonia. The data presented in Fig. 3 represent the most precise data currently available on $p\text{-}\bar{\Lambda}$ and $\Lambda\text{-}\bar{\Lambda}$ pairs and can provide constraints for theoretical models on these interactions.

In conclusion, femtoscopic techniques have been adopted to study the annihilation dynamics in $p\text{-}\bar{p}$, $p\text{-}\bar{\Lambda}$ and $\Lambda\text{-}\bar{\Lambda}$ systems. A quantitative determination of the effective coupling weights, connected to the annihilation channels present in $p\text{-}\bar{p}$, has been obtained adopting a coupled-channel approach with N³LO χ EFT potentials [11]. The largest couplings have been obtained in the spin triplet P (3P_0) and singlet S (1S_0) state. The inclusion of these inelastic channels leads to a better agreement between data and model in the region of k^* below 50 MeV/c, indicating a wide presence of annihilation channels close to threshold. The scattering parameters obtained in Pb–Pb collisions [23] have been used to model the $p\text{-}\bar{\Lambda}$ and $\Lambda\text{-}\bar{\Lambda}$ data using the Lednický–Lyuboshits formula. A consistent description of the $\Lambda\text{-}\bar{\Lambda}$ correlation is achieved while an increase of the $\mathcal{I}f_0$ in the $p\text{-}\bar{\Lambda}$ interaction is needed to improve the agreement with the $p\text{-}\bar{\Lambda}$ data. These results, confirmed by kinematics and SU(3) flavor symmetry considerations, indicate

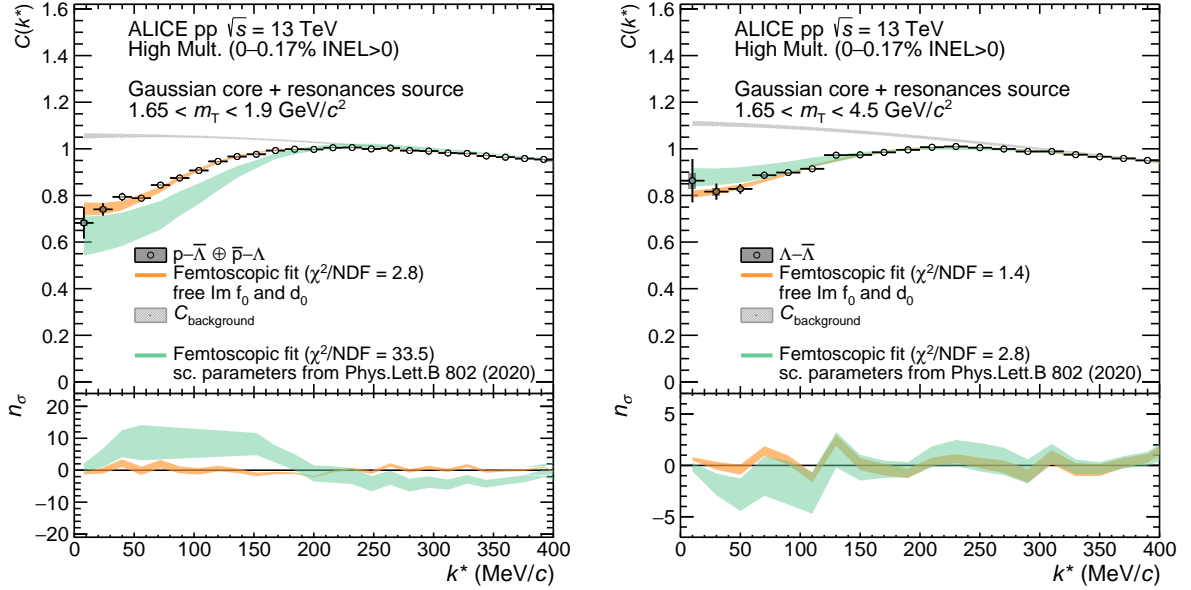


Figure 3: (Color online) Measured correlation function of $p\text{-}\bar{\Lambda}$ (left) and $\Lambda\text{-}\bar{\Lambda}$ (right) pairs for two representative m_T bins. Statistical (bars) and systematic (boxes) uncertainties are shown separately. Results using the Lednický–Lyuboshits formula with Pb–Pb scattering parameters [23] are shown in light green. Orange bands are the results with d_0 and $\mathcal{I}f_0$ as free parameters. In grey the corresponding $C_{\text{background}}(k^*)$, multiplied by the normalization constant N_D , is shown. The reported average χ^2/NDF is evaluated in the k^* interval $[0, 400]$ MeV/c and it includes correlations between the data points. Lower panel: same as in Fig. 2.

a larger contribution in $p\text{-}\bar{\Lambda}$ from annihilation channels in comparison to $\Lambda\text{-}\bar{\Lambda}$. The ALICE data shown in this work delivered the most precise measurements on $p\text{-}\bar{p}$, $p\text{-}\bar{\Lambda}$ and $\Lambda\text{-}\bar{\Lambda}$ systems at low momenta and suggest that baryonia are unlikely to occur in $p\text{-}\bar{p}$ and $p\text{-}\bar{\Lambda}$ systems due to the large annihilation contributions present for these pairs. A modeling of the $B\text{-}\bar{B}$ interaction for systems as $p\text{-}\bar{\Lambda}$, based on optical potentials, and a quantitative estimate of production of the multi-meson annihilation channels in the collisions, can provide a better understanding of the elastic and the annihilation term which can help to strengthen final conclusions on possible bound states.

Acknowledgements

The ALICE Collaboration is grateful to Prof. Johann Haidenbauer and Prof. Francesco Giacosa for the extremely valuable guidance on the theoretical aspects and fruitful discussions.

The ALICE Collaboration would like to thank all its engineers and technicians for their invaluable contributions to the construction of the experiment and the CERN accelerator teams for the outstanding performance of the LHC complex. The ALICE Collaboration gratefully acknowledges the resources and support provided by all Grid centres and the Worldwide LHC Computing Grid (WLCG) collaboration. The ALICE Collaboration acknowledges the following funding agencies for their support in building and running the ALICE detector: A. I. Alikhanyan National Science Laboratory (Yerevan Physics Institute) Foundation (ANSL), State Committee of Science and World Federation of Scientists (WFS), Armenia; Austrian Academy of Sciences, Austrian Science Fund (FWF): [M 2467-N36] and Nationalstiftung für Forschung, Technologie und Entwicklung, Austria; Ministry of Communications and High Technologies, National Nuclear Research Center, Azerbaijan; Conselho Nacional de Desenvolvimento Científico e Tecnológico (CNPq), Financiadora de Estudos e Projetos (Finep), Fundação de Amparo à Pesquisa do Estado de São Paulo (FAPESP) and Universidade Federal do Rio Grande do Sul (UFRGS), Brazil; Ministry of Education of China (MOEC), Ministry of Science & Technology of China (MSTC) and National

Natural Science Foundation of China (NSFC), China; Ministry of Science and Education and Croatian Science Foundation, Croatia; Centro de Aplicaciones Tecnológicas y Desarrollo Nuclear (CEADEN), Cubaenergía, Cuba; Ministry of Education, Youth and Sports of the Czech Republic, Czech Republic; The Danish Council for Independent Research — Natural Sciences, the VILLUM FONDEN and Danish National Research Foundation (DNRF), Denmark; Helsinki Institute of Physics (HIP), Finland; Commissariat à l’Energie Atomique (CEA) and Institut National de Physique Nucléaire et de Physique des Particules (IN2P3) and Centre National de la Recherche Scientifique (CNRS), France; Bundesministerium für Bildung und Forschung (BMBF) and GSI Helmholtzzentrum für Schwerionenforschung GmbH, Germany; General Secretariat for Research and Technology, Ministry of Education, Research and Religions, Greece; National Research, Development and Innovation Office, Hungary; Department of Atomic Energy Government of India (DAE), Department of Science and Technology, Government of India (DST), University Grants Commission, Government of India (UGC) and Council of Scientific and Industrial Research (CSIR), India; Indonesian Institute of Science, Indonesia; Istituto Nazionale di Fisica Nucleare (INFN), Italy; Institute for Innovative Science and Technology, Nagasaki Institute of Applied Science (IIST), Japanese Ministry of Education, Culture, Sports, Science and Technology (MEXT) and Japan Society for the Promotion of Science (JSPS) KAKENHI, Japan; Consejo Nacional de Ciencia (CONACYT) y Tecnología, through Fondo de Cooperación Internacional en Ciencia y Tecnología (FONCICYT) and Dirección General de Asuntos del Personal Académico (DGAPA), Mexico; Nederlandse Organisatie voor Wetenschappelijk Onderzoek (NWO), Netherlands; The Research Council of Norway, Norway; Commission on Science and Technology for Sustainable Development in the South (COMSATS), Pakistan; Pontificia Universidad Católica del Perú, Peru; Ministry of Education and Science, National Science Centre and WUT ID-UB, Poland; Korea Institute of Science and Technology Information and National Research Foundation of Korea (NRF), Republic of Korea; Ministry of Education and Scientific Research, Institute of Atomic Physics and Ministry of Research and Innovation and Institute of Atomic Physics, Romania; Joint Institute for Nuclear Research (JINR), Ministry of Education and Science of the Russian Federation, National Research Centre Kurchatov Institute, Russian Science Foundation and Russian Foundation for Basic Research, Russia; Ministry of Education, Science, Research and Sport of the Slovak Republic, Slovakia; National Research Foundation of South Africa, South Africa; Swedish Research Council (VR) and Knut & Alice Wallenberg Foundation (KAW), Sweden; European Organization for Nuclear Research, Switzerland; Suranaree University of Technology (SUT), National Science and Technology Development Agency (NSDTA) and Office of the Higher Education Commission under NRU project of Thailand, Thailand; Turkish Energy, Nuclear and Mineral Research Agency (TENMAK), Turkey; National Academy of Sciences of Ukraine, Ukraine; Science and Technology Facilities Council (STFC), United Kingdom; National Science Foundation of the United States of America (NSF) and United States Department of Energy, Office of Nuclear Physics (DOE NP), United States of America.

In addition, individual groups and members have received support from Horizon 2020 and Marie Skłodowska Curie Actions, European Union.

References

- [1] O. Chamberlain *et al.*, “Example of an Anti-proton Nucleon Annihilation”, *Phys. Rev.* **102** (1956) 921–923.
- [2] C. Amsler and F. Myhrer, “Low-energy anti-proton physics”, *Ann. Rev. Nucl. Part. Sci.* **41** (1991) 219–267.
- [3] C. B. Dover, T. Gutsche, M. Maruyama, and A. Faessler, “The Physics of nucleon - anti-nucleon annihilation”, *Prog. Part. Nucl. Phys.* **29** (1992) 87–174.
- [4] D. Zhou and R. G. E. Timmermans, “Energy-dependent partial-wave analysis of all antiproton-proton scattering data below 925 MeV/c”, *Phys. Rev.* **C86** (2012) 044003,

- arXiv:1210.7074 [hep-ph].
- [5] E. Klempt, F. Bradamante, A. Martin, and J. M. Richard, “Antinucleon–nucleon interaction at low energy: Scattering and protonium”, *Phys. Rept.* **368** (2002) 119–316.
- [6] B. Loiseau and S. Wycech, “Extraction of baryonia from the lightest antiprotonic atoms”, *Phys. Rev.* **C102** (2020) 034006, arXiv:2007.01775 [nucl-th].
- [7] **BES** Collaboration, J. Z. Bai *et al.*, “Observation of a near threshold enhancement in the p anti- p mass spectrum from radiative $J/\psi \rightarrow \gamma p\bar{p}$ decays”, *Phys. Rev. Lett.* **91** (2003) 022001, arXiv:hep-ex/0303006.
- [8] **BaBar** Collaboration, B. Aubert *et al.*, “Measurement of the $B^+ \rightarrow p\bar{p}K^+$ branching fraction and study of the decay dynamics”, *Phys. Rev.* **D72** (2005) 051101, arXiv:hep-ex/0507012.
- [9] **BaBar** Collaboration, B. Aubert *et al.*, “A Study of $e^+e^- \rightarrow p\bar{p}$ using initial state radiation with BABAR”, *Phys. Rev.* **D73** (2006) 012005, arXiv:hep-ex/0512023.
- [10] **BESIII** Collaboration, M. Ablikim *et al.*, “Spin-Parity Analysis of $p\bar{p}$ Mass Threshold Structure in J/ψ and ψ' Radiative Decays”, *Phys. Rev. Lett.* **108** (2012) 112003, arXiv:1112.0942 [hep-ex].
- [11] L.-Y. Dai, J. Haidenbauer, and U.-G. Meißner, “Antinucleon-nucleon interaction at next-to-next-to-next-to-leading order in chiral effective field theory”, *JHEP* **07** (2017) 078, arXiv:1702.02065 [nucl-th].
- [12] T. Hippchen, J. Haidenbauer, K. Holinde, and V. Mull, “Meson - baryon dynamics in the nucleon - anti-nucleon system. 1. The Nucleon - anti-nucleon interaction”, *Phys. Rev.* **C44** (1991) 1323–1336.
- [13] V. Mull, J. Haidenbauer, T. Hippchen, and K. Holinde, “Meson - baryon dynamics in the nucleon - anti-nucleon system. 2. Annihilation into two mesons”, *Phys. Rev.* **C44** (1991) 1337–1353.
- [14] B. El-Bennich, M. Lacombe, B. Loiseau, and S. Wycech, “Paris N anti-N potential constrained by recent antiprotonic-atom data and antineutron-proton total cross sections”, *Phys. Rev.* **C79** (2009) 054001, arXiv:0807.4454 [nucl-th].
- [15] D. R. Entem and F. Fernandez, “The N anti-N interaction in a constituent quark model: Baryonium states and protonium level shifts”, *Phys. Rev.* **C73** (2006) 045214.
- [16] J. Haidenbauer, K. Holinde, V. Mull, and J. Speth, “Meson exchange and quark - gluon transitions in the $\bar{p}p \rightarrow \bar{\Lambda}\Lambda$ process”, *Phys. Rev.* **C46** (1992) 2158–2171.
- [17] R. G. E. Timmermans, T. A. Rijken, and J. J. de Swart, “Strangeness exchange in anti-proton proton scattering”, *Phys. Rev.* **D45** (1992) 2288–2307.
- [18] J. Haidenbauer, T. Hippchen, K. Holinde, B. Holzenkamp, V. Mull, and J. Speth, “The Reaction $\bar{p}p \rightarrow \bar{\Lambda}\Lambda$ in the meson exchange picture”, *Phys. Rev.* **C45** (1992) 931–946.
- [19] J. Haidenbauer, K. Holinde, and J. Speth, “The $\bar{p}p \rightarrow \bar{\Xi}\Xi$ reaction in the meson exchange picture”, *Phys. Rev.* **C47** (1993) 2982–2985.
- [20] **GlueX** Collaboration, S. Adhikari *et al.*, “The GLUEX beamline and detector”, *Nucl. Instrum. Meth.* **A 987** (2021) 164807, arXiv:2005.14272 [physics.ins-det].
- [21] A. Kisiel, H. Zbroszczyk, and M. Szymański, “Extracting baryon-antibaryon strong interaction potentials from $p\bar{\Lambda}$ femtoscopic correlation functions”, *Phys. Rev.* **C89** (2014) 054916, arXiv:1403.0433 [nucl-th].
- [22] E. Seifert and W. Cassing, “Baryon-antibaryon annihilation and reproduction in relativistic heavy-ion collisions”, *Phys. Rev.* **C97** (2018) 024913, arXiv:1710.00665 [hep-ph].
- [23] **ALICE** Collaboration, S. Acharya *et al.*, “Measurement of strange baryon–antibaryon interactions with femtoscopic correlations”, *Phys. Lett.* **B802** (2020) 135223, arXiv:1903.06149 [nucl-ex].
- [24] **STAR** Collaboration, J. Adams *et al.*, “ p - Λ correlations in central Au+Au collisions at

- $\sqrt{s_{NN}} = 200$ GeV”, *Phys. Rev.* **C74** (2006) 064906, arXiv:nuc1-ex/0511003.
- [25] ALICE Collaboration, S. Acharya *et al.*, “p-p, p- Λ and Λ - Λ correlations studied via femtoscopy in pp reactions at $\sqrt{s} = 7$ TeV”, *Phys. Rev.* **C99** (2019) 024001, arXiv:1805.12455 [nucl-ex].
- [26] ALICE Collaboration, S. Acharya *et al.*, “Study of the Λ - Λ interaction with femtoscopy correlations in pp and p-Pb collisions at the LHC”, *Phys. Lett.* **B 797** (2019) 134822, arXiv:1905.07209 [nucl-ex].
- [27] ALICE Collaboration, S. Acharya *et al.*, “Scattering studies with low-energy kaon-proton femtoscopy in proton-proton collisions at the LHC”, *Phys. Rev. Lett.* **124** (2020) 092301, arXiv:1905.13470 [nucl-ex].
- [28] ALICE Collaboration, S. Acharya *et al.*, “First Observation of an Attractive Interaction between a Proton and a Cascade Baryon”, *Phys. Rev. Lett.* **123** (2019) 112002, arXiv:1904.12198 [nucl-ex].
- [29] ALICE Collaboration, S. Acharya *et al.*, “Investigation of the p- Σ^0 interaction via femtoscopy in pp collisions”, *Phys. Lett.* **B 805** (2020) 135419, arXiv:1910.14407 [nucl-ex].
- [30] ALICE Collaboration, S. Acharya *et al.*, “Unveiling the strong interaction among hadrons at the LHC”, *Nature* **588** (2020) 232–238.
- [31] ALICE Collaboration, S. Acharya *et al.*, “Search for a common baryon source in high-multiplicity pp collisions at the LHC”, *Phys. Lett. B* **811** (2020) 135849, arXiv:2004.08018 [nucl-ex].
- [32] Y. Kamiya, T. Hyodo, K. Morita, A. Ohnishi, and W. Weise, “ $K^- p$ Correlation Function from High-Energy Nuclear Collisions and Chiral SU(3) Dynamics”, *Phys. Rev. Lett.* **124** (2020) 132501, arXiv:1911.01041 [nucl-th].
- [33] J. Haidenbauer, “Coupled-channel effects in hadron-hadron correlation functions”, *Nucl. Phys.* **A981** (2019) 1–16, arXiv:1808.05049 [hep-ph].
- [34] ALICE Collaboration, K. Aamodt *et al.*, “The ALICE experiment at the CERN LHC”, *J. Instr.* **3** (2008) S08002.
- [35] ALICE Collaboration, B. Abelev *et al.*, “Performance of the ALICE experiment at the CERN LHC”, *Int. J. Mod. Phys.* **A29** (2014) 1430044.
- [36] ALICE Collaboration, E. Abbas *et al.*, “Performance of the ALICE VZERO system”, *J. Instrum.* **8** (2013) P10016–P10016.
- [37] ALICE Collaboration, K. Aamodt *et al.*, “Alignment of the ALICE Inner Tracking System with cosmic-ray tracks”, *JINST* **5** (2010) P03003, arXiv:1001.0502 [physics.ins-det].
- [38] J. Alme, Y. Andres, H. Appelshäuser, S. Bablok, N. Bialas, *et al.*, “The ALICE TPC, a large 3-dimensional tracking device with fast readout for ultra-high multiplicity events”, *Nucl.Instrum.Meth.* **A622** (2010) 316–367, arXiv:1001.1950 [physics.ins-det].
- [39] A. Akindinov *et al.*, “Performance of the ALICE Time-Of-Flight detector at the LHC”, *Eur. Phys. J. Plus* **128** (2013) 44.
- [40] Particle Data Group Collaboration, M. Tanabashi *et al.*, “Review of Particle Physics”, *Phys. Rev.* **D98** (2018) 030001.
- [41] M. A. Lisa, S. Pratt, R. Soltz, and U. Wiedemann, “Femtoscopy in relativistic heavy ion collisions”, *Ann. Rev. Nucl. Part. Sci.* **55** (2005) 357–402, arXiv:nuc1-ex/0505014.
- [42] R. Lednický and V. Lyuboshits, “Final State Interaction Effect on Pairing Correlations Between Particles with Small Relative Momenta”, *Sov. J. Nucl. Phys.* **35** (1982) 770.
- [43] V. Vovchenko and H. Stoecker, “Thermal-FIST: A package for heavy-ion collisions and hadronic equation of state”, *Comput. Phys. Commun.* **244** (2019) 295–310, arXiv:1901.05249 [nucl-th].
- [44] T. Pierog, I. Karpenko, J. Katzy, E. Yatsenko, and K. Werner, “EPOS LHC: Test of collective hadronization with data measured at the CERN Large Hadron Collider”, *Phys. Rev.* **C92** (2015)

- 034906, arXiv:1306.0121 [hep-ph].
- [45] ALICE Collaboration, S. Acharya *et al.*, “Kaon–proton strong interaction at low relative momentum via femtoscopy in Pb–Pb collisions at the LHC”, *Phys. Lett. B* **822** (2021) 136708, arXiv:2105.05683 [nucl-ex].
- [46] L. Fabbietti, V. M. Sarti, and O. V. Doce, “Study of the strong interaction among hadrons with correlations at the LHC”, *Ann. Rev. Nucl. Part. Sci.* **71** (2021) 377–402, arXiv:2012.09806 [nucl-ex].
- [47] D. Mihaylov, V. Mantovani Sarti, O. Arnold, L. Fabbietti, B. Hohlweger, and A. Mathis, “A femtoscopic Correlation Analysis Tool using the Schrödinger equation (CATS)”, *Eur. Phys. J. C* **78** (2018) 394, arXiv:1802.08481 [hep-ph].
- [48] J. Haidenbauer, C. Hanhart, X.-W. Kang, and U.-G. Meißner, “Origin of the structures observed in e^+e^- annihilation into multipion states around the $\bar{p}p$ threshold”, *Phys. Rev.* **D92** (2015) 054032, arXiv:1506.08120 [nucl-th].
- [49] ARGUS Collaboration, H. Albrecht *et al.*, “Observation of Octet and Decuplet Hyperons in e^+e^- Annihilation at 10-GeV Center-of-mass Energy”, *Phys. Lett. B* **183** (1987) 419–424.
- [50] M. W. Sullivan *et al.*, “Measurement of the Ratio of Σ^0 to Λ^0 Inclusive Production From 28.5-GeV/c Protons on Beryllium”, *Phys. Rev.* **D36** (1987) 674.
- [51] B. S. Yuldashev *et al.*, “Neutral strange particle production in p Ne-20 and p N interactions at 300-GeV/c”, *Phys. Rev.* **D43** (1991) 2792–2802.
- [52] T. Sjöstrand *et al.*, “An Introduction to PYTHIA 8.2”, *Comput. Phys. Commun.* **191** (2015) 159–177.
- [53] L. Olbrich, M. Zétényi, F. Giacosa, and D. H. Rischke, “Three-flavor chiral effective model with four baryonic multiplets within the mirror assignment”, *Phys. Rev.* **D93** (2016) 034021, arXiv:1511.05035 [hep-ph].
- [54] C. J. Batty, “ANTI-PROTONIC HYDROGEN ATOMS”, *Rept. Prog. Phys.* **52** (1989) 1165–1216.
- [55] B. O. Kerbikov and A. E. Kudryavtsev, “Singlet spin fraction in p anti-p and the proton form-factor at threshold”, *Nucl. Phys. A* **558** (1993) 177C–182C.
- [56] M. Pignone, M. Lacombe, B. Loiseau, and R. Vinh Mau, “Paris N anti-N potential and recent proton anti-proton low-energy data”, *Phys. Rev. C* **50** (1994) 2710–2730.

A Additional material

A.1 $p-\bar{\Lambda}$ and $\Lambda-\bar{\Lambda}$ results in m_T intervals

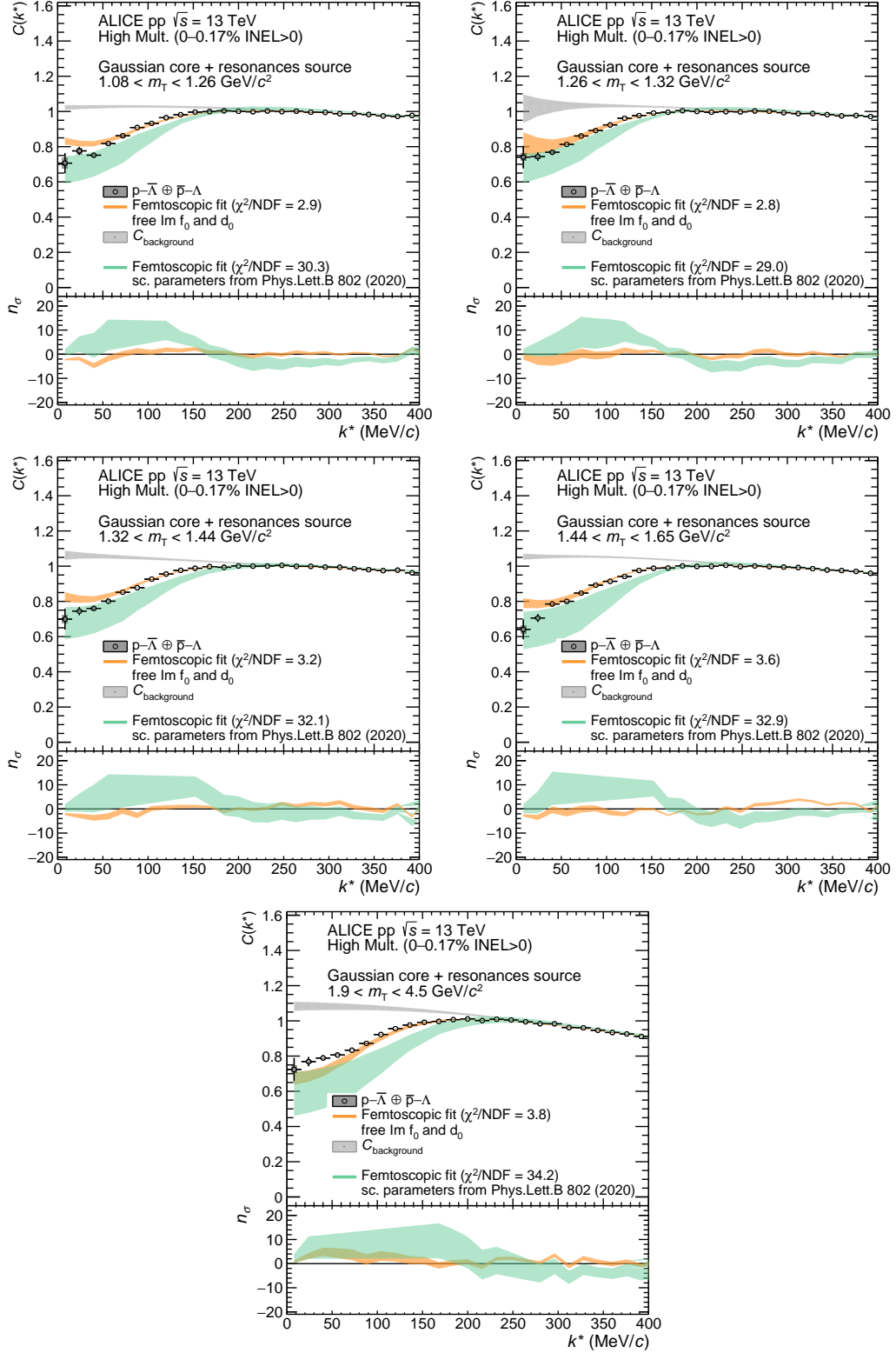


Figure A.1: (Color online) Measured correlation function of $p-\bar{\Lambda}$ pairs for remaining m_T bins. Same description as in Fig. 3.

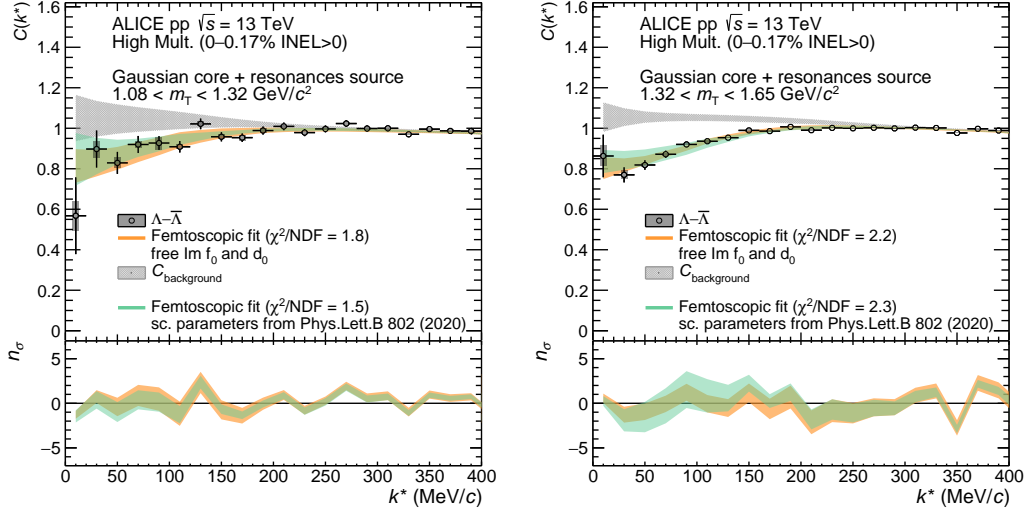


Figure A.2: (Color online) Measured correlation function of Λ – $\bar{\Lambda}$ pairs for remaining m_T bins. Same description as in Fig. 3.

A.2 Results on p – \bar{p} pairs with the Lednický–Lyuboshits model

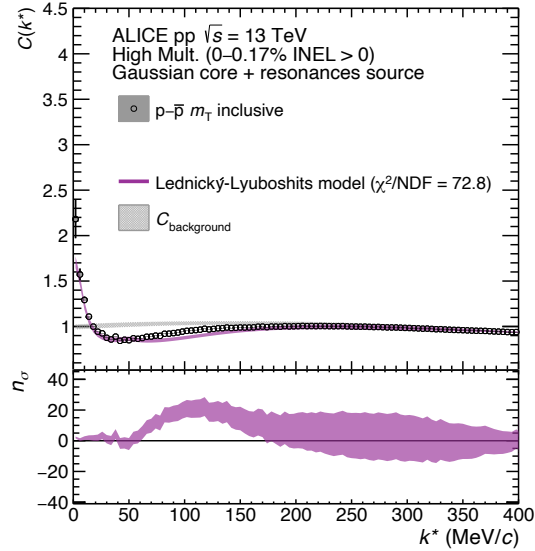


Figure A.3: (Color online) Measured correlation function of p – \bar{p} pairs. Statistical (bars) and systematic (boxes) uncertainties are shown separately. The results assuming the Lednický–Lyuboshits model with Coulomb included, as in [23], are shown by the violet band. The scattering parameters used as input for the Lednický–Lyuboshits calculations include only the n – \bar{n} contribution as coupled-channel [54–56]. The model completely underestimates the k^* region from 50 to 150 MeV/c. As can be seen in Fig. 2, the annihilation channels play a role in this intermediate region and a better description of the data is achieved when using the Migdal–Watson approximation to include them. This is a clear indication that the multi-meson channels are explicitly needed to model the current measured p – \bar{p} correlation function. The Lednický–Lyuboshits calculation also overestimates the coupling to the n – \bar{n} channel, as can be seen from the large cusp structure at $k^* \approx 50$ MeV/c not present in the data. Lower panel: n_σ deviation between data and model in terms of numbers of statistical standard deviations.

B The ALICE Collaboration

S. Acharya¹⁴³, D. Adamová⁹⁸, A. Adler⁷⁶, J. Adolfsson⁸³, G. Aglieri Rinella³⁵, M. Agnello³¹, N. Agrawal⁵⁵, Z. Ahammed¹⁴³, S. Ahmad¹⁶, S.U. Ahn⁷⁸, I. Ahuja³⁹, Z. Akbar⁵², A. Akindinov⁹⁵, M. Al-Turany¹¹⁰, S.N. Alam⁴¹, D. Aleksandrov⁹¹, B. Alessandro⁶¹, H.M. Alfanda⁷, R. Alfaro Molina⁷³, B. Ali¹⁶, Y. Ali¹⁴, A. Alici²⁶, N. Alizadehvandchali¹²⁷, A. Alkin³⁵, J. Alme²¹, T. Alt⁷⁰, L. Altenkamper²¹, I. Altsybeev¹¹⁵, M.N. Anaam⁷, C. Andrei⁴⁹, D. Andreou⁹³, A. Andronic¹⁴⁶, M. Angeletti³⁵, V. Anguelov¹⁰⁷, F. Antinori⁵⁸, P. Antonioli⁵⁵, C. Anuj¹⁶, N. Apadula⁸², L. Aphecetche¹¹⁷, H. Appelshäuser⁷⁰, S. Arcelli²⁶, R. Arnaldi⁶¹, I.C. Arsene²⁰, M. Arslanodk^{148,107}, A. Augustinus³⁵, R. Averbeck¹¹⁰, S. Aziz⁸⁰, M.D. Azmi¹⁶, A. Badala⁵⁷, Y.W. Baek⁴², X. Bai^{131,110}, R. Bailhache⁷⁰, Y. Bailung⁵¹, R. Bala¹⁰⁴, A. Balbino³¹, A. Baldisseri¹⁴⁰, B. Balis², M. Ball⁴⁴, D. Banerjee⁴, R. Barbera²⁷, L. Barioglio^{108,25}, M. Barlou⁸⁷, G.G. Barnaföldi¹⁴⁷, L.S. Barnby⁹⁷, V. Barret¹³⁷, C. Bartels¹³⁰, K. Barth³⁵, E. Bartsch⁷⁰, F. Baruffaldi²⁸, N. Bastid¹³⁷, S. Basu⁸³, G. Batigne¹¹⁷, B. Batyunya⁷⁷, D. Bauri⁵⁰, J.L. Bazo Alba¹¹⁴, I.G. Bearden⁹², C. Beattie¹⁴⁸, I. Belikov¹³⁹, A.D.C. Bell Hechavarria¹⁴⁶, F. Bellini^{26,35}, R. Bellwied¹²⁷, S. Belokurova¹¹⁵, V. Belyaev⁹⁶, G. Bencedi⁷¹, S. Beole²⁵, A. Bercuci⁴⁹, Y. Berdnikov¹⁰¹, A. Berdnikova¹⁰⁷, D. Berenyi¹⁴⁷, L. Bergmann¹⁰⁷, M.G. Besoiu⁶⁹, L. Betev³⁵, P.P. Bhaduri¹⁴³, A. Bhasin¹⁰⁴, I.R. Bhat¹⁰⁴, M.A. Bhat⁴, B. Bhattacharjee⁴³, P. Bhattacharya²³, L. Bianchi²⁵, N. Bianchi⁵³, J. Bielčik³⁸, J. Bielčíková⁹⁸, J. Biernat¹²⁰, A. Bilandzic¹⁰⁸, G. Biro¹⁴⁷, S. Biswas⁴, J.T. Blair¹²¹, D. Blau⁹¹, M.B. Blidaru¹¹⁰, C. Blume⁷⁰, G. Boca^{29,59}, F. Bock⁹⁹, A. Bogdanov⁹⁶, S. Boi²³, J. Bok⁶³, L. Boldizsár¹⁴⁷, A. Bolozdynya⁹⁶, M. Bombara³⁹, P.M. Bond³⁵, G. Bonomi^{142,59}, H. Borel¹⁴⁰, A. Borissov⁸⁴, H. Bossi¹⁴⁸, E. Botta²⁵, L. Bratrud⁷⁰, P. Braun-Munzinger¹¹⁰, M. Bregant¹²³, M. Broz³⁸, G.E. Bruno^{109,34}, M.D. Buckland¹³⁰, D. Budnikov¹¹¹, H. Buesching⁷⁰, S. Bufalino³¹, O. Bugnon¹¹⁷, P. Buhler¹¹⁶, Z. Buthelezi^{74,134}, J.B. Butt¹⁴, S.A. Bysiak¹²⁰, D. Caffarri⁹³, M. Cai^{28,7}, H. Caines¹⁴⁸, A. Caliva¹¹⁰, E. Calvo Villar¹¹⁴, J.M.M. Camacho¹²², R.S. Camacho⁴⁶, P. Camerini²⁴, F.D.M. Canedo¹²³, F. Carnesecchi^{35,26}, R. Caron¹⁴⁰, J. Castillo Castellanos¹⁴⁰, E.A.R. Casula²³, F. Catalano³¹, C. Ceballos Sanchez⁷⁷, P. Chakraborty⁵⁰, S. Chandra¹⁴³, S. Chapeland³⁵, M. Chartier¹³⁰, S. Chattopadhyay¹⁴³, S. Chattopadhyay¹¹², A. Chauvin²³, T.G. Chavez⁴⁶, C. Cheshkov¹³⁸, B. Cheynis¹³⁸, V. Chibante Barroso³⁵, D.D. Chinellato¹²⁴, S. Cho⁶³, P. Chochula³⁵, P. Christakoglou⁹³, C.H. Christensen⁹², P. Christiansen⁸³, T. Chujo¹³⁶, C. Cicalo⁵⁶, L. Cifarelli²⁶, F. Cindolo⁵⁵, M.R. Ciupek¹¹⁰, G. Clai^{II,55}, J. Cleymans^{I,126}, F. Colamaria⁵⁴, J.S. Colburn¹¹³, D. Colella^{109,54,34,147}, A. Collu⁸², M. Colocci^{35,26}, M. Concas^{III,61}, G. Conesa Balbastre⁸¹, Z. Conesa del Valle⁸⁰, G. Contin²⁴, J.G. Contreras³⁸, M.L. Coquet¹⁴⁰, T.M. Cormier⁹⁹, P. Cortese³², M.R. Cosentino¹²⁵, F. Costa³⁵, S. Costanza^{29,59}, P. Crochet¹³⁷, E. Cuautle⁷¹, P. Cui⁷, L. Cunqueiro⁹⁹, A. Dainese⁵⁸, F.P.A. Damas^{117,140}, M.C. Danisch¹⁰⁷, A. Danu⁶⁹, I. Das¹¹², P. Das⁸⁹, P. Das⁴, S. Das⁴, S. Dash⁵⁰, S. De⁸⁹, A. De Caro³⁰, G. de Cataldo⁵⁴, L. De Cilladi²⁵, J. de Cuveland⁴⁰, A. De Falco²³, D. De Gruttola³⁰, N. De Marco⁶¹, C. De Martin²⁴, S. De Pasquale³⁰, S. Deb⁵¹, H.F. Degenhardt¹²³, K.R. Deja¹⁴⁴, L. Dello Stritto³⁰, S. Delsanto²⁵, W. Deng⁷, P. Dhankher¹⁹, D. Di Bari³⁴, A. Di Mauro³⁵, R.A. Diaz⁸, T. Dietel¹²⁶, Y. Ding^{138,7}, R. Divià³⁵, D.U. Dixit¹⁹, Ø. Djuvsland²¹, U. Dmitrieva⁶⁵, J. Do⁶³, A. Dobrin⁶⁹, B. Dönigus⁷⁰, O. Dordic²⁰, A.K. Dubey¹⁴³, A. Dubla^{110,93}, S. Dudi¹⁰³, M. Dukhishyam⁸⁹, P. Dupieux¹³⁷, N. Dzalaiova¹³, T.M. Eder¹⁴⁶, R.J. Ehlers⁹⁹, V.N. Eikeland²¹, D. Elia⁵⁴, B. Erazmus¹¹⁷, F. Ercolessi²⁶, F. Erhardt¹⁰², A. Erokhin¹¹⁵, M.R. Ersdal²¹, B. Espagnon⁸⁰, G. Eulisse³⁵, D. Evans¹¹³, S. Evdokimov⁹⁴, L. Fabbietti¹⁰⁸, M. Faggin²⁸, J. Faivre⁸¹, F. Fan⁷, A. Fantoni⁵³, M. Fasel⁹⁹, P. Fedichio³¹, A. Feliciello⁶¹, G. Feofilov¹¹⁵, A. Fernández Téllez⁴⁶, A. Ferrero¹⁴⁰, A. Ferretti²⁵, V.J.G. Feuillard¹⁰⁷, J. Figiel¹²⁰, S. Filchagin¹¹¹, D. Finogeev⁶⁵, F.M. Fionda^{56,21}, G. Fiorenza^{35,109}, F. Flor¹²⁷, A.N. Flores¹²¹, S. Foertsch⁷⁴, P. Foka¹¹⁰, S. Fokin⁹¹, E. Fragiaco⁶², E. Frajna¹⁴⁷, U. Fuchs³⁵, N. Funicello³⁰, C. Furget⁸¹, A. Furs⁶⁵, J.J. Gaardhøje⁹², M. Gagliardi²⁵, A.M. Gago¹¹⁴, A. Gal¹³⁹, C.D. Galvan¹²², P. Ganoti⁸⁷, C. Garabatos¹¹⁰, J.R.A. Garcia⁴⁶, E. Garcia-Solis¹⁰, K. Garg¹¹⁷, C. Gargiulo³⁵, A. Garibli⁹⁰, K. Garner¹⁴⁶, P. Gasik¹¹⁰, E.F. Gauger¹²¹, A. Gautam¹²⁹, M.B. Gay Ducati⁷², M. Germain¹¹⁷, J. Ghosh¹¹², P. Ghosh¹⁴³, S.K. Ghosh⁴, M. Giacalone²⁶, P. Gianotti⁵³, P. Giubellino^{110,61}, P. Giubilato²⁸, A.M.C. Glaenger¹⁴⁰, P. Glässel¹⁰⁷, D.J.Q. Goh⁸⁵, V. Gonzalez¹⁴⁵, L.H. González-Trueba⁷³, S. Gorbunov⁴⁰, M. Gorgon², L. Görlich¹²⁰, S. Gotovac³⁶, V. Grabski⁷³, L.K. Graczykowski¹⁴⁴, L. Greiner⁸², A. Grelli⁶⁴, C. Grigoras³⁵, V. Grigoriev⁹⁶, A. Grigoryan^{I,1}, S. Grigoryan^{77,1}, O.S. Groettvik²¹, F. Grosa^{35,61}, J.F. Grosse-Oetringhaus³⁵, R. Grosso¹¹⁰, G.G. Guardiano¹²⁴, R. Guernane⁸¹, M. Guilbaud¹¹⁷, K. Gulbrandsen⁹², T. Gunji¹³⁵, A. Gupta¹⁰⁴, R. Gupta¹⁰⁴, I.B. Guzman⁴⁶, S.P. Guzman⁴⁶, L. Gyulai¹⁴⁷, M.K. Habib¹¹⁰, C. Hadjidakis⁸⁰, G. Halimoglu⁷⁰, H. Hamagaki⁸⁵, G. Hamar¹⁴⁷, M. Hamid⁷, R. Hannigan¹²¹, M.R. Haque^{144,89}, A. Harlanderova¹¹⁰, J.W. Harris¹⁴⁸, A. Harton¹⁰, J.A. Hasenbichler³⁵, H. Hassan⁹⁹, D. Hatzifotiadou⁵⁵, P. Hauer⁴⁴, L.B. Havener¹⁴⁸, S. Hayashi¹³⁵, S.T. Heckel¹⁰⁸, E. Hellbär⁷⁰, H. Helstrup³⁷, T. Herman³⁸, E.G. Hernandez⁴⁶, G. Herrera Corral⁹, F. Herrmann¹⁴⁶, K.F. Hetland³⁷, H. Hillemanns³⁵, C. Hills¹³⁰, B. Hippolyte¹³⁹, B. Hofman⁶⁴, B. Hohlweger^{93,108}, J. Honermann¹⁴⁶, G.H. Hong¹⁴⁹, D. Horak³⁸, S. Hornung¹¹⁰, A. Horzyk², R. Hosokawa¹⁵, P. Hristov³⁵, C. Huang⁸⁰, C. Hughes¹³³, P. Huhn⁷⁰, T.J. Humanic¹⁰⁰, H. Hushnud¹¹², L.A. Husova¹⁴⁶, A. Hutson¹²⁷, D. Hutter⁴⁰, J.P. Iddon^{35,130},

R. Ilkaev¹¹¹, H. Ilyas¹⁴, M. Inaba¹³⁶, G.M. Innocenti³⁵, M. Ippolitov⁹¹, A. Isakov^{38,98}, M.S. Islam¹¹², M. Ivanov¹¹⁰, V. Ivanov¹⁰¹, V. Izucheev⁹⁴, M. Jablonski², B. Jacak⁸², N. Jacazio³⁵, P.M. Jacobs⁸², S. Jadlovská¹¹⁹, J. Jadlovsky¹¹⁹, S. Jaelani⁶⁴, C. Jahnke^{124,123}, M.J. Jakubowska¹⁴⁴, M.A. Janik¹⁴⁴, T. Janson⁷⁶, M. Jercic¹⁰², O. Jevons¹¹³, F. Jonas^{99,146}, P.G. Jones¹¹³, J.M. Jowett^{35,110}, J. Jung⁷⁰, M. Jung⁷⁰, A. Junique³⁵, A. Jusko¹¹³, J. Kaewjai¹¹⁸, P. Kalinak⁶⁶, A. Kalweit³⁵, V. Kaplin⁹⁶, S. Kar⁷, A. Karasu Uysal⁷⁹, D. Karatovic¹⁰², O. Karavichev⁶⁵, T. Karavicheva⁶⁵, P. Karczmarczyk¹⁴⁴, E. Karpechev⁶⁵, A. Kazantsev⁹¹, U. Keschull⁷⁶, R. Keidel⁴⁸, D.L.D. Keijdener⁶⁴, M. Keil³⁵, B. Ketzer⁴⁴, Z. Khabanova⁹³, A.M. Khan⁷, S. Khan¹⁶, A. Khanzadeev¹⁰¹, Y. Kharlov⁹⁴, A. Khatun¹⁶, A. Khuntia¹²⁰, B. Kileng³⁷, B. Kim^{17,63}, D. Kim¹⁴⁹, D.J. Kim¹²⁸, E.J. Kim⁷⁵, J. Kim¹⁴⁹, J.S. Kim⁴², J. Kim¹⁰⁷, J. Kim¹⁴⁹, J. Kim⁷⁵, M. Kim¹⁰⁷, S. Kim¹⁸, T. Kim¹⁴⁹, S. Kirsch⁷⁰, I. Kisel⁴⁰, S. Kiselev⁹⁵, A. Kisiel¹⁴⁴, J.P. Kitowski², J.L. Klay⁶, J. Klein³⁵, S. Klein⁸², C. Klein-Bösing¹⁴⁶, M. Kleiner⁷⁰, T. Klemenz¹⁰⁸, A. Kluge³⁵, A.G. Knospe¹²⁷, C. Kobdaj¹¹⁸, M.K. Köhler¹⁰⁷, T. Kollegger¹¹⁰, A. Kondratyev⁷⁷, N. Kondratyeva⁹⁶, E. Kondratyuk⁹⁴, J. König⁷⁰, S.A. Königstorfer¹⁰⁸, P.J. Konopka^{35,2}, G. Kornakov¹⁴⁴, S.D. Koryciak², L. Koska¹¹⁹, A. Kotliarov⁹⁸, O. Kovalenko⁸⁸, V. Kovalenko¹¹⁵, M. Kowalski¹²⁰, I. Králik⁶⁶, A. Kravčáková³⁹, L. Kreis¹¹⁰, M. Krivda^{113,66}, F. Krizek⁹⁸, K. Krizkova Gajdosova³⁸, M. Kroesen¹⁰⁷, M. Krüger⁷⁰, E. Kryshen¹⁰¹, M. Krzewicki⁴⁰, V. Kučera³⁵, C. Kuhn¹³⁹, P.G. Kuijer⁹³, T. Kumaoka¹³⁶, D. Kumar¹⁴³, L. Kumar¹⁰³, N. Kumar¹⁰³, S. Kundu^{35,89}, P. Kurashvili⁸⁸, A. Kurepin⁶⁵, A.B. Kurepin⁶⁵, A. Kuryakin¹¹¹, S. Kuschpil⁹⁸, J. Kvapil¹¹³, M.J. Kweon⁶³, J.Y. Kwon⁶³, Y. Kwon¹⁴⁹, S.L. La Pointe⁴⁰, P. La Rocca²⁷, Y.S. Lai⁸², A. Lakrathok¹¹⁸, M. Lamanna³⁵, R. Langoy¹³², K. Lapidus³⁵, P. Larionov⁵³, E. Laudi³⁵, L. Lautner^{35,108}, R. Lavicka³⁸, T. Lazareva¹¹⁵, R. Lea^{142,24,59}, J. Lee¹³⁶, J. Lehrbach⁴⁰, R.C. Lemmon⁹⁷, I. León Monzón¹²², E.D. Lesser¹⁹, M. Lettrich^{35,108}, P. Lévai¹⁴⁷, X. Li¹¹, X.L. Li⁷, J. Lien¹³², R. Lietava¹¹³, B. Lim¹⁷, S.H. Lim¹⁷, V. Lindenstruth⁴⁰, A. Lindner⁴⁹, C. Lippmann¹¹⁰, A. Liu¹⁹, J. Liu¹³⁰, I.M. Lofnes²¹, V. Loginov⁹⁶, C. Loizides⁹⁹, P. Loncar³⁶, J.A. Lopez¹⁰⁷, X. Lopez¹³⁷, E. López Torres⁸, J.R. Luhder¹⁴⁶, M. Lunardon²⁸, G. Luparello⁶², Y.G. Ma⁴¹, A. Maevskaya⁶⁵, M. Mager³⁵, T. Mahmoud⁴⁴, A. Maire¹³⁹, M. Malaev¹⁰¹, Q.W. Malik²⁰, L. Malinina^{14,77}, D. Mal'Kevich⁹⁵, N. Mallick⁵¹, P. Malzacher¹¹⁰, G. Mandaglio^{33,57}, V. Manko⁹¹, F. Manso¹³⁷, V. Manzari⁵⁴, Y. Mao⁷, J. Mareš⁶⁸, G.V. Margagliotti²⁴, A. Margotti⁵⁵, A. Marín¹¹⁰, C. Markert¹²¹, M. Marquard⁷⁰, N.A. Martin¹⁰⁷, P. Martinengo³⁵, J.L. Martinez¹²⁷, M.I. Martínez⁴⁶, G. Martínez García¹¹⁷, S. Masciocchi¹¹⁰, M. Masera²⁵, A. Masoni⁵⁶, L. Massacrier⁸⁰, A. Mastroserio^{141,54}, A.M. Mathis¹⁰⁸, O. Matonoha⁸³, P.F.T. Matuoka¹²³, A. Matyja¹²⁰, C. Mayer¹²⁰, A.L. Mazuecos³⁵, F. Mazzaschi²⁵, M. Mazzilli³⁵, M.A. Mazzoni⁶⁰, J.E. Mdhluli¹³⁴, A.F. Mechler⁷⁰, F. Meddi²², Y. Melikyan⁶⁵, A. Menchaca-Rocha⁷³, E. Meninno^{116,30}, A.S. Menon¹²⁷, M. Meres¹³, S. Mhlanga^{126,74}, Y. Miake¹³⁶, L. Micheletti^{61,25}, L.C. Migliorin¹³⁸, D.L. Mihaylov¹⁰⁸, K. Mikhaylov^{77,95}, A.N. Mishra¹⁴⁷, D. Miśkowiec¹¹⁰, A. Modak⁴, A.P. Mohanty⁶⁴, B. Mohanty⁸⁹, M. Mohisin Khan¹⁶, Z. Moravcova⁹², C. Mordasini¹⁰⁸, D.A. Moreira De Godoy¹⁴⁶, L.A.P. Moreno⁴⁶, I. Morozov⁶⁵, A. Morsch³⁵, T. Mrnjavac³⁵, V. Muccifora⁵³, E. Mudnic³⁶, D. Mühlheim¹⁴⁶, S. Muhuri¹⁴³, J.D. Mulligan⁸², A. Mulliri²³, M.G. Munhoz¹²³, R.H. Munzer⁷⁰, H. Murakami¹³⁵, S. Murray¹²⁶, L. Musa³⁵, J. Musinsky⁶⁶, C.J. Myers¹²⁷, J.W. Myrcha¹⁴⁴, B. Naik^{134,50}, R. Nair⁸⁸, B.K. Nandi⁵⁰, R. Nania⁵⁵, E. Nappi⁵⁴, M.U. Naru¹⁴, A.F. Nassirpour⁸³, A. Nath¹⁰⁷, C. Natrass¹³³, A. Neagu²⁰, L. Nellen⁷¹, S.V. Nesbo³⁷, G. Neskovic⁴⁰, D. Nesterov¹¹⁵, B.S. Nielsen⁹², S. Nikolaev⁹¹, S. Nikulin⁹¹, V. Nikulin¹⁰¹, F. Noferini⁵⁵, S. Noh¹², P. Nomokonov⁷⁷, J. Norman¹³⁰, N. Novitzky¹³⁶, P. Nowakowski¹⁴⁴, A. Nyman⁹¹, J. Nystrand²¹, M. Ogino⁸⁵, A. Ohlson⁸³, V.A. Okorokov⁹⁶, J. Oleniacz¹⁴⁴, A.C. Oliveira Da Silva¹³³, M.H. Oliver¹⁴⁸, A. Onnerstad¹²⁸, C. Oppedisano⁶¹, A. Ortiz Velasquez⁷¹, T. Osako⁴⁷, A. Oskarsson⁸³, J. Otwinowski¹²⁰, K. Oyama⁸⁵, Y. Pachmayer¹⁰⁷, S. Padhan⁵⁰, D. Pagano^{142,59}, G. Paic⁷¹, A. Palasciano⁵⁴, J. Pan¹⁴⁵, S. Panebianco¹⁴⁰, P. Pareek¹⁴³, J. Park⁶³, J.E. Parkkila¹²⁸, S.P. Pathak¹²⁷, R.N. Patra^{104,35}, B. Paul²³, J. Pazzini^{142,59}, H. Pei⁷, T. Peitzmann⁶⁴, X. Peng⁷, L.G. Pereira⁷², H. Pereira Da Costa¹⁴⁰, D. Peresunko⁹¹, G.M. Perez⁸, S. Perrin¹⁴⁰, Y. Pestov⁵, V. Petráček³⁸, M. Petrovici⁴⁹, R.P. Pezzi⁷², S. Piano⁶², M. Pikna¹³, P. Pillot¹¹⁷, O. Pinazza^{55,35}, L. Pinsky¹²⁷, C. Pinto²⁷, S. Pisano⁵³, M. Płoskoń⁸², M. Planinic¹⁰², F. Pliquett⁷⁰, M.G. Poghosyan⁹⁹, B. Polichtchouk⁹⁴, S. Politano³¹, N. Poljak¹⁰², A. Pop⁴⁹, S. Porteboeuf-Houssais¹³⁷, J. Porter⁸², V. Pozdniakov⁷⁷, S.K. Prasad⁴, R. Preghenella⁵⁵, F. Prino⁶¹, C.A. Pruneau¹⁴⁵, I. Pshenichnov⁶⁵, M. Puccio³⁵, S. Qiu⁹³, L. Quaglia²⁵, R.E. Quishpe¹²⁷, S. Ragoni¹¹³, A. Rakotozafindrabe¹⁴⁰, L. Ramello³², F. Rami¹³⁹, S.A.R. Ramirez⁴⁶, A.G.T. Ramos³⁴, T.A. Rancien⁸¹, R. Raniwala¹⁰⁵, S. Raniwala¹⁰⁵, S.S. Räsänen⁴⁵, R. Rath⁵¹, I. Ravasenga⁹³, K.F. Read^{99,133}, A.R. Redelbach⁴⁰, K. Redlich^{5,88}, A. Rehman²¹, P. Reichelt⁷⁰, F. Reidt³⁵, H.A. Reme-ness³⁷, R. Renfordt⁷⁰, Z. Rescakova³⁹, K. Reygers¹⁰⁷, A. Riabov¹⁰¹, V. Riabov¹⁰¹, T. Richert^{83,92}, M. Richter²⁰, W. Riegler³⁵, F. Riggi²⁷, C. Ristea⁶⁹, S.P. Rode⁵¹, M. Rodríguez Cahuantzi⁴⁶, K. Røed²⁰, R. Rogalev⁹⁴, E. Rogochaya⁷⁷, T.S. Rogoschinski⁷⁰, D. Rohr³⁵, D. Röhrich²¹, P.F. Rojas⁴⁶, P.S. Rokita¹⁴⁴, F. Ronchetti⁵³, A. Rosano^{33,57}, E.D. Rosas⁷¹, A. Rossi⁵⁸, A. Rotondi^{29,59}, A. Roy⁵¹, P. Roy¹¹², S. Roy⁵⁰, N. Rubini²⁶, O.V. Rueda⁸³, R. Rui²⁴, B. Rumyantsev⁷⁷, P.G. Russek², A. Rustamov⁹⁰, E. Ryabinkin⁹¹, Y. Ryabov¹⁰¹, A. Rybicki¹²⁰, H. Ryttonen¹²⁸, W. Rzesza¹⁴⁴, O.A.M. Saarimaki⁴⁵, R. Sadek¹¹⁷, S. Sadovsky⁹⁴,

J. Saetre²¹, K. Šafařík³⁸, S.K. Saha¹⁴³, S. Saha⁸⁹, B. Sahoo⁵⁰, P. Sahoo⁵⁰, R. Sahoo⁵¹, S. Sahoo⁶⁷, D. Sahu⁵¹, P.K. Sahu⁶⁷, J. Saini¹⁴³, S. Sakai¹³⁶, S. Sambyal¹⁰⁴, V. Samsonov^{1,101,96}, D. Sarkar¹⁴⁵, N. Sarkar¹⁴³, P. Sarma⁴³, V.M. Sarti¹⁰⁸, M.H.P. Sas¹⁴⁸, J. Schambach^{99,121}, H.S. Scheid⁷⁰, C. Schiaua⁴⁹, R. Schicker¹⁰⁷, A. Schmah¹⁰⁷, C. Schmidt¹¹⁰, H.R. Schmidt¹⁰⁶, M.O. Schmidt¹⁰⁷, M. Schmidt¹⁰⁶, N.V. Schmidt^{99,70}, A.R. Schmier¹³³, R. Schotter¹³⁹, J. Schukraft³⁵, Y. Schutz¹³⁹, K. Schwarz¹¹⁰, K. Schweda¹¹⁰, G. Scioli²⁶, E. Scomparin⁶¹, J.E. Seger¹⁵, Y. Sekiguchi¹³⁵, D. Sekihata¹³⁵, I. Selyuzhenkov^{110,96}, S. Senyukov¹³⁹, J.J. Seo⁶³, D. Serebryakov⁶⁵, L. Šeršnyté¹⁰⁸, A. Sevcenco⁶⁹, T.J. Shaba⁷⁴, A. Shabanov⁶⁵, A. Shabetai¹¹⁷, R. Shahoyan³⁵, W. Shaikh¹¹², A. Shangaraev⁹⁴, A. Sharma¹⁰³, H. Sharma¹²⁰, M. Sharma¹⁰⁴, N. Sharma¹⁰³, S. Sharma¹⁰⁴, O. Sheibani¹²⁷, K. Shigaki⁴⁷, M. Shimomura⁸⁶, S. Shirinkin⁹⁵, Q. Shou⁴¹, Y. Sibiriyak⁹¹, S. Siddhanta⁵⁶, T. Siemiarczuk⁸⁸, T.F. Silva¹²³, D. Silvermyr⁸³, G. Simonetti³⁵, B. Singh¹⁰⁸, R. Singh⁸⁹, R. Singh¹⁰⁴, R. Singh⁵¹, V.K. Singh¹⁴³, V. Singhal¹⁴³, T. Sinha¹¹², B. Sitar¹³, M. Sitta³², T.B. Skaali²⁰, G. Skorodumovs¹⁰⁷, M. Slupecki⁴⁵, N. Smirnov¹⁴⁸, R.J.M. Snellings⁶⁴, C. Soncco¹¹⁴, J. Song¹²⁷, A. Songmoolnak¹¹⁸, F. Soramel²⁸, S. Sorensen¹³³, I. Sputowska¹²⁰, J. Stachel¹⁰⁷, I. Stan⁶⁹, P.J. Steffanic¹³³, S.F. Stiefelmaier¹⁰⁷, D. Stocco¹¹⁷, I. Storehaug²⁰, M.M. Storetvedt³⁷, C.P. Stylianidis⁹³, A.A.P. Suaide¹²³, T. Sugitate⁴⁷, C. Suire⁸⁰, M. Suljic³⁵, R. Sultanov⁹⁵, M. Šumbera⁹⁸, V. Sumberia¹⁰⁴, S. Sumowidagdo⁵², S. Swain⁶⁷, A. Szabo¹³, I. Szarka¹³, U. Tabassam¹⁴, S.F. Taghavi¹⁰⁸, G. Taillepiet¹³⁷, J. Takahashi¹²⁴, G.J. Tambave²¹, S. Tang^{137,7}, Z. Tang¹³¹, M. Tarhini¹¹⁷, M.G. Tarzila⁴⁹, A. Tauro³⁵, G. Tejada Muñoz⁴⁶, A. Telesca³⁵, L. Terlizzi²⁵, C. Terrevoli¹²⁷, G. Tersimonov³, S. Thakur¹⁴³, D. Thomas¹²¹, R. Tieulent¹³⁸, A. Tikhonov⁶⁵, A.R. Timmins¹²⁷, M. Tkacik¹¹⁹, A. Toia⁷⁰, N. Topilskaya⁶⁵, M. Toppi⁵³, F. Torales-Acosta¹⁹, T. Tork⁸⁰, R.C. Torres⁸², S.R. Torres³⁸, A. Trifiro^{33,57}, S. Tripathy^{55,71}, T. Tripathy⁵⁰, S. Trogolo^{35,28}, G. Trombetta³⁴, V. Trubnikov³, W.H. Trzaska¹²⁸, T.P. Trzcinski¹⁴⁴, B.A. Trzeciak³⁸, A. Tumkin¹¹¹, R. Turrisi⁵⁸, T.S. Tveter²⁰, K. Ullaland²¹, A. Uras¹³⁸, M. Urioni^{59,142}, G.L. Usai²³, M. Vala³⁹, N. Valle^{59,29}, S. Vallerio⁶¹, N. van der Kolk⁶⁴, L.V.R. van Doremalen⁶⁴, M. van Leeuwen⁹³, R.J.G. van Weelden⁹³, P. Vande Vyvre³⁵, D. Varga¹⁴⁷, Z. Varga¹⁴⁷, M. Varga-Kofarago¹⁴⁷, A. Vargas⁴⁶, M. Vasileiou⁸⁷, A. Vasiliev⁹¹, O. Vázquez Doce¹⁰⁸, V. Vechernin¹¹⁵, E. Vercellin²⁵, S. Vergara Limón⁴⁶, L. Vermunt⁶⁴, R. Vértesi¹⁴⁷, M. Verweij⁶⁴, L. Vickovic³⁶, Z. Vilakazi¹³⁴, O. Villalobos Baillie¹¹³, G. Vino⁵⁴, A. Vinogradov⁹¹, T. Virgili³⁰, V. Vislavicius⁹², A. Vodopyanov⁷⁷, B. Volkel³⁵, M.A. Völkl¹⁰⁷, K. Voloshin⁹⁵, S.A. Voloshin¹⁴⁵, G. Volpe³⁴, B. von Haller³⁵, I. Vorobyev¹⁰⁸, D. Voscek¹¹⁹, J. Vrláková³⁹, B. Wagner²¹, C. Wang⁴¹, D. Wang⁴¹, M. Weber¹¹⁶, A. Wegrzynek³⁵, S.C. Wenzel³⁵, J.P. Wessels¹⁴⁶, J. Wiechula⁷⁰, J. Wikne²⁰, G. Wilk⁸⁸, J. Wilkinson¹¹⁰, G.A. Willems¹⁴⁶, B. Windelband¹⁰⁷, M. Winn¹⁴⁰, W.E. Witt¹³³, J.R. Wright¹²¹, W. Wu⁴¹, Y. Wu¹³¹, R. Xu⁷, S. Yalcin⁷⁹, Y. Yamaguchi⁴⁷, K. Yamakawa⁴⁷, S. Yang²¹, S. Yano^{47,140}, Z. Yin⁷, H. Yokoyama⁶⁴, I.-K. Yoo¹⁷, J.H. Yoon⁶³, S. Yuan²¹, A. Yuncu¹⁰⁷, V. Zaccolo²⁴, A. Zaman¹⁴, C. Zampolli³⁵, H.J.C. Zanoli⁶⁴, N. Zardoshti³⁵, A. Zarochentsev¹¹⁵, P. Závada⁶⁸, N. Zaviyalov¹¹¹, H. Zbroszczyk¹⁴⁴, M. Zhalov¹⁰¹, S. Zhang⁴¹, X. Zhang⁷, Y. Zhang¹³¹, V. Zhrebchevskii¹¹⁵, Y. Zhi¹¹, D. Zhou⁷, Y. Zhou⁹², J. Zhu^{7,110}, Y. Zhu⁷, A. Zichichi²⁶, G. Zinovjev³, N. Zurlo^{142,59}

Affiliation notes

^I Deceased

^{II} Also at: Italian National Agency for New Technologies, Energy and Sustainable Economic Development (ENEA), Bologna, Italy

^{III} Also at: Dipartimento DET del Politecnico di Torino, Turin, Italy

^{IV} Also at: M.V. Lomonosov Moscow State University, D.V. Skobeltsyn Institute of Nuclear, Physics, Moscow, Russia

^V Also at: Institute of Theoretical Physics, University of Wrocław, Poland

Collaboration Institutes

¹ A.I. Alikhanyan National Science Laboratory (Yerevan Physics Institute) Foundation, Yerevan, Armenia

² AGH University of Science and Technology, Cracow, Poland

³ Bogolyubov Institute for Theoretical Physics, National Academy of Sciences of Ukraine, Kiev, Ukraine

⁴ Bose Institute, Department of Physics and Centre for Astroparticle Physics and Space Science (CAPSS), Kolkata, India

⁵ Budker Institute for Nuclear Physics, Novosibirsk, Russia

⁶ California Polytechnic State University, San Luis Obispo, California, United States

⁷ Central China Normal University, Wuhan, China

⁸ Centro de Aplicaciones Tecnológicas y Desarrollo Nuclear (CEADEN), Havana, Cuba

- ⁹ Centro de Investigación y de Estudios Avanzados (CINVESTAV), Mexico City and Mérida, Mexico
- ¹⁰ Chicago State University, Chicago, Illinois, United States
- ¹¹ China Institute of Atomic Energy, Beijing, China
- ¹² Chungbuk National University, Cheongju, Republic of Korea
- ¹³ Comenius University Bratislava, Faculty of Mathematics, Physics and Informatics, Bratislava, Slovakia
- ¹⁴ COMSATS University Islamabad, Islamabad, Pakistan
- ¹⁵ Creighton University, Omaha, Nebraska, United States
- ¹⁶ Department of Physics, Aligarh Muslim University, Aligarh, India
- ¹⁷ Department of Physics, Pusan National University, Pusan, Republic of Korea
- ¹⁸ Department of Physics, Sejong University, Seoul, Republic of Korea
- ¹⁹ Department of Physics, University of California, Berkeley, California, United States
- ²⁰ Department of Physics, University of Oslo, Oslo, Norway
- ²¹ Department of Physics and Technology, University of Bergen, Bergen, Norway
- ²² Dipartimento di Fisica dell'Università 'La Sapienza' and Sezione INFN, Rome, Italy
- ²³ Dipartimento di Fisica dell'Università and Sezione INFN, Cagliari, Italy
- ²⁴ Dipartimento di Fisica dell'Università and Sezione INFN, Trieste, Italy
- ²⁵ Dipartimento di Fisica dell'Università and Sezione INFN, Turin, Italy
- ²⁶ Dipartimento di Fisica e Astronomia dell'Università and Sezione INFN, Bologna, Italy
- ²⁷ Dipartimento di Fisica e Astronomia dell'Università and Sezione INFN, Catania, Italy
- ²⁸ Dipartimento di Fisica e Astronomia dell'Università and Sezione INFN, Padova, Italy
- ²⁹ Dipartimento di Fisica e Nucleare e Teorica, Università di Pavia, Pavia, Italy
- ³⁰ Dipartimento di Fisica 'E.R. Caianiello' dell'Università and Gruppo Collegato INFN, Salerno, Italy
- ³¹ Dipartimento DISAT del Politecnico and Sezione INFN, Turin, Italy
- ³² Dipartimento di Scienze e Innovazione Tecnologica dell'Università del Piemonte Orientale and INFN Sezione di Torino, Alessandria, Italy
- ³³ Dipartimento di Scienze MIFT, Università di Messina, Messina, Italy
- ³⁴ Dipartimento Interateneo di Fisica 'M. Merlin' and Sezione INFN, Bari, Italy
- ³⁵ European Organization for Nuclear Research (CERN), Geneva, Switzerland
- ³⁶ Faculty of Electrical Engineering, Mechanical Engineering and Naval Architecture, University of Split, Split, Croatia
- ³⁷ Faculty of Engineering and Science, Western Norway University of Applied Sciences, Bergen, Norway
- ³⁸ Faculty of Nuclear Sciences and Physical Engineering, Czech Technical University in Prague, Prague, Czech Republic
- ³⁹ Faculty of Science, P.J. Šafárik University, Košice, Slovakia
- ⁴⁰ Frankfurt Institute for Advanced Studies, Johann Wolfgang Goethe-Universität Frankfurt, Frankfurt, Germany
- ⁴¹ Fudan University, Shanghai, China
- ⁴² Gangneung-Wonju National University, Gangneung, Republic of Korea
- ⁴³ Gauhati University, Department of Physics, Guwahati, India
- ⁴⁴ Helmholtz-Institut für Strahlen- und Kernphysik, Rheinische Friedrich-Wilhelms-Universität Bonn, Bonn, Germany
- ⁴⁵ Helsinki Institute of Physics (HIP), Helsinki, Finland
- ⁴⁶ High Energy Physics Group, Universidad Autónoma de Puebla, Puebla, Mexico
- ⁴⁷ Hiroshima University, Hiroshima, Japan
- ⁴⁸ Hochschule Worms, Zentrum für Technologietransfer und Telekommunikation (ZTT), Worms, Germany
- ⁴⁹ Horia Hulubei National Institute of Physics and Nuclear Engineering, Bucharest, Romania
- ⁵⁰ Indian Institute of Technology Bombay (IIT), Mumbai, India
- ⁵¹ Indian Institute of Technology Indore, Indore, India
- ⁵² Indonesian Institute of Sciences, Jakarta, Indonesia
- ⁵³ INFN, Laboratori Nazionali di Frascati, Frascati, Italy
- ⁵⁴ INFN, Sezione di Bari, Bari, Italy
- ⁵⁵ INFN, Sezione di Bologna, Bologna, Italy
- ⁵⁶ INFN, Sezione di Cagliari, Cagliari, Italy
- ⁵⁷ INFN, Sezione di Catania, Catania, Italy
- ⁵⁸ INFN, Sezione di Padova, Padova, Italy
- ⁵⁹ INFN, Sezione di Pavia, Pavia, Italy
- ⁶⁰ INFN, Sezione di Roma, Rome, Italy

- 61 INFN, Sezione di Torino, Turin, Italy
- 62 INFN, Sezione di Trieste, Trieste, Italy
- 63 Inha University, Incheon, Republic of Korea
- 64 Institute for Gravitational and Subatomic Physics (GRASP), Utrecht University/Nikhef, Utrecht, Netherlands
- 65 Institute for Nuclear Research, Academy of Sciences, Moscow, Russia
- 66 Institute of Experimental Physics, Slovak Academy of Sciences, Košice, Slovakia
- 67 Institute of Physics, Homi Bhabha National Institute, Bhubaneswar, India
- 68 Institute of Physics of the Czech Academy of Sciences, Prague, Czech Republic
- 69 Institute of Space Science (ISS), Bucharest, Romania
- 70 Institut für Kernphysik, Johann Wolfgang Goethe-Universität Frankfurt, Frankfurt, Germany
- 71 Instituto de Ciencias Nucleares, Universidad Nacional Autónoma de México, Mexico City, Mexico
- 72 Instituto de Física, Universidade Federal do Rio Grande do Sul (UFRGS), Porto Alegre, Brazil
- 73 Instituto de Física, Universidad Nacional Autónoma de México, Mexico City, Mexico
- 74 iThemba LABS, National Research Foundation, Somerset West, South Africa
- 75 Jeonbuk National University, Jeonju, Republic of Korea
- 76 Johann-Wolfgang-Goethe Universität Frankfurt Institut für Informatik, Fachbereich Informatik und Mathematik, Frankfurt, Germany
- 77 Joint Institute for Nuclear Research (JINR), Dubna, Russia
- 78 Korea Institute of Science and Technology Information, Daejeon, Republic of Korea
- 79 KTO Karatay University, Konya, Turkey
- 80 Laboratoire de Physique des 2 Infinis, Irène Joliot-Curie, Orsay, France
- 81 Laboratoire de Physique Subatomique et de Cosmologie, Université Grenoble-Alpes, CNRS-IN2P3, Grenoble, France
- 82 Lawrence Berkeley National Laboratory, Berkeley, California, United States
- 83 Lund University Department of Physics, Division of Particle Physics, Lund, Sweden
- 84 Moscow Institute for Physics and Technology, Moscow, Russia
- 85 Nagasaki Institute of Applied Science, Nagasaki, Japan
- 86 Nara Women's University (NWU), Nara, Japan
- 87 National and Kapodistrian University of Athens, School of Science, Department of Physics, Athens, Greece
- 88 National Centre for Nuclear Research, Warsaw, Poland
- 89 National Institute of Science Education and Research, Homi Bhabha National Institute, Jatni, India
- 90 National Nuclear Research Center, Baku, Azerbaijan
- 91 National Research Centre Kurchatov Institute, Moscow, Russia
- 92 Niels Bohr Institute, University of Copenhagen, Copenhagen, Denmark
- 93 Nikhef, National institute for subatomic physics, Amsterdam, Netherlands
- 94 NRC Kurchatov Institute IHEP, Protvino, Russia
- 95 NRC «Kurchatov» Institute - ITEP, Moscow, Russia
- 96 NRNU Moscow Engineering Physics Institute, Moscow, Russia
- 97 Nuclear Physics Group, STFC Daresbury Laboratory, Daresbury, United Kingdom
- 98 Nuclear Physics Institute of the Czech Academy of Sciences, Řež u Prahy, Czech Republic
- 99 Oak Ridge National Laboratory, Oak Ridge, Tennessee, United States
- 100 Ohio State University, Columbus, Ohio, United States
- 101 Petersburg Nuclear Physics Institute, Gatchina, Russia
- 102 Physics department, Faculty of science, University of Zagreb, Zagreb, Croatia
- 103 Physics Department, Panjab University, Chandigarh, India
- 104 Physics Department, University of Jammu, Jammu, India
- 105 Physics Department, University of Rajasthan, Jaipur, India
- 106 Physikalisches Institut, Eberhard-Karls-Universität Tübingen, Tübingen, Germany
- 107 Physikalisches Institut, Ruprecht-Karls-Universität Heidelberg, Heidelberg, Germany
- 108 Physik Department, Technische Universität München, Munich, Germany
- 109 Politecnico di Bari and Sezione INFN, Bari, Italy
- 110 Research Division and ExtreMe Matter Institute EMMI, GSI Helmholtzzentrum für Schwerionenforschung GmbH, Darmstadt, Germany
- 111 Russian Federal Nuclear Center (VNIIEF), Sarov, Russia
- 112 Saha Institute of Nuclear Physics, Homi Bhabha National Institute, Kolkata, India
- 113 School of Physics and Astronomy, University of Birmingham, Birmingham, United Kingdom

- 114 Sección Física, Departamento de Ciencias, Pontificia Universidad Católica del Perú, Lima, Peru
- 115 St. Petersburg State University, St. Petersburg, Russia
- 116 Stefan Meyer Institut für Subatomare Physik (SMI), Vienna, Austria
- 117 SUBATECH, IMT Atlantique, Université de Nantes, CNRS-IN2P3, Nantes, France
- 118 Suranaree University of Technology, Nakhon Ratchasima, Thailand
- 119 Technical University of Košice, Košice, Slovakia
- 120 The Henryk Niewodniczanski Institute of Nuclear Physics, Polish Academy of Sciences, Cracow, Poland
- 121 The University of Texas at Austin, Austin, Texas, United States
- 122 Universidad Autónoma de Sinaloa, Culiacán, Mexico
- 123 Universidade de São Paulo (USP), São Paulo, Brazil
- 124 Universidade Estadual de Campinas (UNICAMP), Campinas, Brazil
- 125 Universidade Federal do ABC, Santo Andre, Brazil
- 126 University of Cape Town, Cape Town, South Africa
- 127 University of Houston, Houston, Texas, United States
- 128 University of Jyväskylä, Jyväskylä, Finland
- 129 University of Kansas, Lawrence, Kansas, United States
- 130 University of Liverpool, Liverpool, United Kingdom
- 131 University of Science and Technology of China, Hefei, China
- 132 University of South-Eastern Norway, Tonsberg, Norway
- 133 University of Tennessee, Knoxville, Tennessee, United States
- 134 University of the Witwatersrand, Johannesburg, South Africa
- 135 University of Tokyo, Tokyo, Japan
- 136 University of Tsukuba, Tsukuba, Japan
- 137 Université Clermont Auvergne, CNRS/IN2P3, LPC, Clermont-Ferrand, France
- 138 Université de Lyon, CNRS/IN2P3, Institut de Physique des 2 Infinis de Lyon , Lyon, France
- 139 Université de Strasbourg, CNRS, IPHC UMR 7178, F-67000 Strasbourg, France, Strasbourg, France
- 140 Université Paris-Saclay Centre d’Etudes de Saclay (CEA), IRFU, Département de Physique Nucléaire (DPhN), Saclay, France
- 141 Università degli Studi di Foggia, Foggia, Italy
- 142 Università di Brescia, Brescia, Italy
- 143 Variable Energy Cyclotron Centre, Homi Bhabha National Institute, Kolkata, India
- 144 Warsaw University of Technology, Warsaw, Poland
- 145 Wayne State University, Detroit, Michigan, United States
- 146 Westfälische Wilhelms-Universität Münster, Institut für Kernphysik, Münster, Germany
- 147 Wigner Research Centre for Physics, Budapest, Hungary
- 148 Yale University, New Haven, Connecticut, United States
- 149 Yonsei University, Seoul, Republic of Korea